Inorganic Chemistry

ARTICLE

pubs.acs.org/IC

Polymer-Anchored Peroxo Compounds of Vanadium(V) and Molybdenum(VI): Synthesis, Stability, and Their Activities with Alkaline Phosphatase and Catalase

Jeena Jyoti Boruah, Diganta Kalita, Siva Prasad Das, Saurav Paul, and Nashreen S. Islam*

Department of Chemical Sciences, Tezpur University, Tezpur 784028, Assam, India

Supporting Information

ABSTRACT: We generated a series of new polymer-bound peroxo complexes of vanadium(V) and molybdenum(VI) of the type $[VO(O_2)_2(sulfonate)]$—PSS [PSS = poly(sodium 4-styrene sulfonate)] (**PV_3**), $[V_2O_2(O_2)_4(carboxylate)VO(O_2)_2$-(sulfonate)]—PSSM [PSSM = poly(sodium styrene sulfonate-*co*-maleate)] (**PV_4**), $[Mo_2O_2(O_2)_4(carboxylate)]$—PA [PA = poly-(sodium acrylate)] (**PMo_1**), $[MoO(O_2)_2(carboxylate)]$—PMA [PMA = poly(sodium methacrylate)] (**PMo_2**), and $[MoO(O_2)_2$-(amide)]—PAm [PAm = poly(acrylamide)] (**PMo_3**) by reacting V_2O_5 (for **PV_3** and **PV_4**) or H_2MoO_4 (for **PMo_1**, **PMo_2**, and **PMo_3**) with H_2O_2 and the respective water-soluble macromolecular ligand at pH 5−6. The compounds were characterized by elemental analysis (CHN and energy-dispersive X-ray spectroscopy), spectral studies (UV−vis, IR, ^{13}C NMR, ^{51}V NMR, and ^{95} Mo NMR), thermal (TGA) as well as scanning electron micrographs (SEM), and EDX analysis. It has been demonstrated that compounds retain their structural integrity in solutions of a wide range of pH values and are approximately 100 times weaker as substrate to the enzyme catalase relative to H_2O_2, its natural substrate. The effect of the title compounds, along with previously reported compounds $[V_2O_2(O_2)_4(carboxylate)]$—PA (**$PV_1$**) and $[VO(O_2)_2(carboxylate)]$—PMA (**PV_2**) on rabbit intestine alkaline phosphatase (ALP) has been investigated and compared with the effect induced by the free diperoxometallates viz. $Na[VO(O_2)_2(H_2O)]$ (**DPV**), $[MoO(O_2)_2(glycine)(H_2O)]$ (**DMo_1**), and $[MoO(O_2)_2(asparagine)(H_2O)]$ (**DMo_2**). It has been observed that although all the compounds tested are potent inhibitors of the enzyme, the polymer-bound and neat complexes act via distinct mechanisms. Each of the macromolecular compounds is a classical noncompetitive inhibitor of ALP. In contrast, the action of neat pV and heteroligand pMo compounds on the enzyme function is consistent with a mixed type of inhibition.

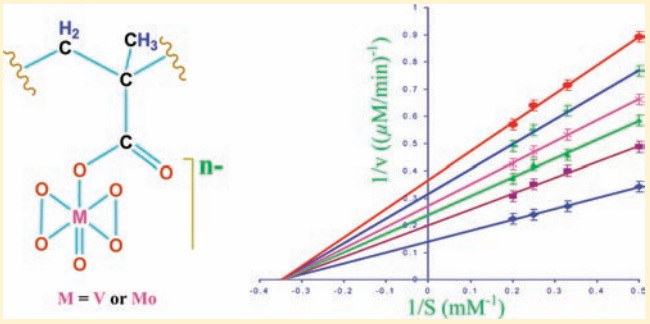

INTRODUCTION

Vanadium and its peroxo compounds are gaining a special status in medicinal inorganic chemistry owing mainly to their enzyme inhibitory,[1] antineoplastic activity[2] and their role as insulin-mimetic agents.[2c,3] Peroxovanadate (pV) compounds are known to affect cellular signaling by affecting the functioning of a number of enzymes such as mitogen-activated protein kinase (MAPkinase), tyrosine phosphatases, and phospholipase D and are reported to cause smooth muscle contraction at a far lower concentration than H_2O_2.[3e,f,4] We have recently shown that sub-optimal doses of sodium antimony gluconate (SAG) and pV compounds are effective in combating infection of mice with antimony resistant *Leishmania donovani*.[5] Apart from peroxovanadates (pV), peroxo compounds of molybdenum (pMo) and tungsten (pW) are now recognized as potential insulin mimics with an ability to inhibit the activity of phosphoproteins.[6] Further, antitumor activity of Mo compounds has been confirmed.[2d,7] Such findings led to a revival of interest in these systems.[6,7,8a]

Although the exact mechanisms involved in most of the metabolic actions of these metals are yet to be fully established, the ability of vanadates to inhibit phosphohydrolase enzymes is recognized as key to understanding the bioactivity of vanadium.[1b,c] There has also been a growing awareness on the importance of enzyme inhibition as a mode of action for inorganic drugs in recent years.[9] One of the ubiquitous groups of phosphohydrolases, nonspecific alkaline phosphatases (ALP), is involved in a variety of biological phenomena and used extensively in immunoassays.[10−12] Oxyanions such as vanadate,[1b] molybdate, and tungstate[13] are, in general, known to be competitive inhibitors of phosphatase enzymes. Reports are also available on the ALP inhibitory activity of pV compounds.[1d,14] However, a majority of the synthetic pV compounds tested for their various biochemical effects suffer from the disadvantage of being not stable enough or toxic,[1d,3b,15] limiting their pharmacological potential. This provided impetus to synthesize new, stable, and structurally defined peroxovanadium complexes.[2c,8] Surprisingly, however, despite the knowledge that aqueous pMo formed

Received: February 21, 2011
Published: July 25, 2011

in a solution of Mo−H_2O_2 are stable in solution,[6] the potential of discrete pMo complexes as biologically active agents remains relatively unexplored.

Recently, we prepared a set of well-defined macrocomplexes by incorporating peroxo vanadium (pV) species into water-soluble polymer matrices viz. poly(sodium acrylate) (**PV_1**) and poly(sodium methacrylate) (**PV_2**).[16] The important features of these polymeric compounds, which appear to be the first known examples of peroxo metal derivatives anchored to water-soluble polymers,[8a] include their high stability in solution, their considerable resistance to degradation by the enzyme catalase,[16] and their bactericidal activity against *E. coli* and *S. aureus*. Moreover, complex **PV_1** containing dimeric pV moieties efficiently catalyzed oxidation of bromide to a bromination-competent intermediate at near neutral pH, an essential requirement of a biomimetic model, whereas free diperoxovanadate compound (**DPV**) as well as **PV_2** with monomeric **DPV** units were inactive in bromination.[16] This finding is significant particularly because, contrary to natural bromoperoxidases which are most efficient at pH 5.5−7, most of the model complexes known so far were found to be catalytically active only in acid medium.[17] During the past decade, our efforts have been directed toward two goals: to develop functional mimics of haloperoxidases with an ability to mediate organic oxidations under mild conditions and to generate peroxometallates with biologically important characteristics.[5,15b,15c,16,18] We observed that even a minor modification of the coordination environment around the pV moieties in the polymeric complexes could alter their bioactivity as well as their catalytic activity tremendously. In order to gain a better understanding of the structure−activity corelation of such systems, in the present study we focused on generating new peroxo metal complexes in diverse macroligand environment. Our specific concern was to explore whether binding of low molecular weight peroxo metal species to macromolecular ligands would alter their affinity as enzyme inhibitors or enhance their resistance to catalase action.

The modification of organic polymers by attaching transition metal complexes constitutes an active area of current research.[19] The utility of water-soluble polymers as supports in organic chemistry and biology is increasingly being recognized in recent years.[20] Polymers often lack many inconvenient properties of monomeric species, such as lability, volatility, toxicity, and odor.[19a] Binding of active drug molecules including low molecular weight metal complexes to soluble macromolecular carriers is of importance since such systems can be expected to overcome the limitations such as toxic side effects by improving the body distribution of drugs and prolonging their activity.[19k,21] Notwithstanding the enormous progress in the field of metal-containing polymers, there appears to be a dearth of information pertaining to the synthesis and testing of biochemical or catalytic properties of peroxometal compounds anchored to water-soluble polymers.

Here, we present the preparation and characterization of a set of new peroxo complexes of the metals, vanadium and molybdenum, anchored to a number of different soluble polymer matrices. Keeping in view the contemporary interest in development of pharmaceutical formulations consisting of acrylic acid and styrene sulfonic acid-based polymers[22,23] and their derivatives and owing to their convenient method of preparation or commercial availability, chemical stability, and presence of appropriate functional groups for easy attachment of metal complexes, we selected, for the purpose of this investigation, polymers viz. poly(sodium acrylate) (PA), poly(sodium methacrylate) (PMA), poly(acrylamide) (PAm), and poly(sodium 4-styrene sulfonate) (PSS) and a copolymer poly(sodium styrene sulfonate-*co*-maleate) (PSSM) as supports. Findings of our investigation on the stability of the compounds, their inhibitory effect on alkaline phosphatase, and interaction with catalase vis-a-vis free mononuclear peroxo compounds of V(V) and two of the known heteroligand peroxo complexes of Mo(VI) are also reported herein.

EXPERIMENTAL SECTION

Materials. The chemicals used were all reagent-grade products. The sources of chemicals are given below: V_2O_5 (SRL, India), molybdic acid (E. Merck, Mumbai, India), poly(sodium acrylate) (M_w = 2100) (Fluka), poly(sodium methacrylate) (M_w = 4000), poly(sodium 4-styrene sulfonate) (M_w = 2 00 000), poly(sodium styrene sulfonate-*co*-maleate) (M_w = 20 000), alkaline phosphatase from rabbit intestine (ALP), catalase and *p*-nitrophenyl phosphate (*p*-NPP) (Sigma-Aldrich Chemical Co., Milwaukee, USA), acrylamide (CDH, New Delhi, India), and sodium thiosulphate, potassium hydrogen phosphate, potassium dihydrogen phosphate, glycine, oxine, and $MgCl_2$ (SD Fine Chemicals, Mumbai, India). $Na[VO(O_2)_2(H_2O)]$ (**DPV**), $[V_2O_2(O_2)_4(carboxylate)]$−PA (**$PV_1$**), and $[VO(O_2)_2(carboxylate)]$−PMA (**PV_2**) were prepared by the method described in our earlier papers.[15c,16] $[MoO(O_2)_2(glycine)(H_2O)]$ (**DMo_1**) and $[MoO(O_2)_2(asparagine)(H_2O)]$ (**DMo_2**) were synthesized according to a previously reported procedure.[24] Polyacrylamide (PAm) was prepared by solution polymerization technique using iron(II) ammonium sulfate and hydrogen peroxide as redox initiator.[25]

Synthesis of $[VO(O_2)_2(sulfonate)]$−PSS (PV_3) and $[V_2O_2(O_2)_4$-(carboxylate)$VO(O_2)_2(sulfonate)]$−PSSM (PV_4). The procedure developed consisted of gradual addition of 12 mL of H_2O_2 (30% solution, 105.84 mmol) to a mixture of V_2O_5 (0.25 g, 1.3 mmol) and 2 mL of 30% PSS (for **PV_3**) or 1.0 g of PSSM (for **PV_4**) dissolved in a minimum volume of water with continuous stirring. Keeping the temperature below −5 °C in an ice−acetone bath, the mixture was stirred for ca. 30 min until all solids dissolved. The reaction solution spontaneously attained a pH of ca. 3 at this stage. Concentrated sodium hydroxide (ca. 8 M) was added dropwise with constant stirring to raise the pH of the reaction medium finally to ca. 6. On adding precooled acetone (ca. 50 mL) to this mixture under vigorous stirring a yellow-colored pasty mass separated out. After allowing it to stand for 20 min in the ice bath, the supernatant liquid was decanted and the residue was treated repeatedly with acetone under scratching until it became a microcrystalline solid. The product was separated by centrifugation, washed with cold acetone, and dried in vacuo over concentrated sulfuric acid. The compounds were further dried by heating up to 70 °C under nitrogen atmosphere.

Synthesis of $[Mo_2O_2(O_2)_4(carboxylate)]$−PA ($PMo_1$), $[MoO(O_2)_2(carboxylate)]$−PMA ($PMo_2$), and $[MoO(O_2)_2(amide)]$−PAm (PMo_3). In a typical reaction, molybdic acid (0.64 g, 4.0 mmol for compounds **PMo_1** and **PMo_2**; 3.4 g, 21.12 mmol for **PMo_3**) was dissolved in 30% H_2O_2 (12 mL, 105.84 mmol for **PMo_1** and **PMo_2**; 22 mL, 194.11 mmol for **PMo_3**) by maintaining the temperature at 30−40 °C. To the clear solution obtained, 1.5 g of the respective polymer was added in portions with continuous stirring. The mixture was stirred for ca. 60 min in an ice bath until all solids dissolved. At this stage the pH of the reaction medium was recorded to be ca. 2. The pH of the solution was raised to ca. 5 by dropwise addition of concentrated NaOH solution (ca. 8 M) with constant stirring. A red-colored pasty mass separated out on adding precooled acetone (ca. 50 mL) to this mixture under vigorous stirring. After being allowed to stand for about 30 min, the supernatant liquid was decanted and the residue was treated repeatedly with acetone under scratching. The microcrystalline product was separated by centrifugation, washed with cold acetone, and dried in vacuo over concentrated sulfuric acid. The compounds were subsequently dried by heating up to 70 °C under nitrogen atmosphere.

dx.doi.org/10.1021/ic200368g |*Inorg. Chem.* 2011, 50, 8046–8062

Elemental Analysis. The compounds were analyzed for C, H, and N by using an elemental analyzer Perkin-Elmer 2400 series II. Vanadium was determined volumetrically by the method described in earlier papers,[26] and molybdenum content was estimated gravimetrically as molybdenum oxinate,[27] $MoO_2(C_9H_6ON)_2$. Peroxide content for the compounds was determined by adding a weighed amount of the compound to a cold solution of 1.5% boric acid (W/V) in 0.7 M sulfuric acid (100 mL) and titration with standard cerium(IV) solution.[26]

Physical and Spectroscopic Measurements. The IR spectra were recorded with samples as KBr pellets in a Nicolet model 410 FT-IR spectrophotometer. The spectra were recorded at ambient temperature by making pressed pellets of the compounds. Spectroscopic determinations of the initial rate of ALP catalyzed hydrolysis of *p*-NPP were carried out in a Cary model Bio 100 spectrophotometer, equipped with a Peltier-controlled constant temperature cell. The absorbance values were denoted as, e.g., A_{405} at the wavelength indicated. SEM characterization was carried out by using a JEOL JSM-6390LV Scanning Electron Micrograph attached with an energy-dispersive X-ray detector. Scanning was done in the 10−20 μM range, and images were taken at a magnification of 15−20 kV. Data were obtained using INCA software. Standardization of the data analysis is an integral part of the SEM-EDX instrument employed. The ^{13}C NMR spectra were recorded on a JEOL JNM-ECS400 spectrometer at a carbon frequency of 100.5 MHz, 131 072 X-resolution points, number of scans 8000, 1.04 s acquisition time, and 2.0 s relaxation delay with the ^{1}H NMR decoupling method in D_2O. ^{51}V NMR spectra were recorded on a Bruker AVANCE II 400 FT spectrometer at a vanadium frequency of 105.25 MHz with the samples in a 10 mm spinning tube with a sealed coaxial tube containing D_2O, which provided the lock signal. Chemical shift data are recorded as negative values of ppm (δ) in the low-frequency direction with reference to $VOCl_3$ at 296 K. The ^{95} Mo NMR spectra were recorded in a Bruker AV 400 MHz FT-NMR spectrometer at a molybdenum frequency of 26.07 MHz with samples in a 10 mm spinning tube with a sealed coaxial tube containing D_2O, which provided the lock signal. The chemical shift data are recorded as negative values of ppm (δ) in the low-frequency direction with reference to 1 M $Na_2MoO_4 \cdot 2H_2O$ solution at 298 K. Magnetic susceptibilities of the complexes were measured by the Gouy method, using Hg[Co(NCS)] as the calibrant. Thermogravimetric analysis was done on a Perkin-Elmer STA 6000 system at a heating rate of 10 °C/min under an atmosphere of nitrogen using an aluminum pan. Prior to TGA analysis, the samples were dried by heating under a nitrogen atmosphere at 70 °C.

Stability of the Complexes Toward Decomposition in Solution. The stability of the compounds in distilled water, at their natural pH, was studied by determining the peroxide content in aliquots drawn from the respective solution of the compound containing **PV$_3$** (0.099 mg/mL), **PV$_4$** (0.116 mg/mL), **PMo$_1$** (0.137 mg/mL), **PMo$_2$** (0.294 mg/mL), **PMo$_3$** (0.327 mg/mL), **DMo$_1$** (0.054 mg/mL), or **DMo$_2$** (0.065 mg/mL) at different intervals of time by the method already described above. The initial peroxide concentration in each of the test solutions was maintained at 0.4 mM. As a measure of the stability of the compounds in solution, changes in the absorbance of their electronic spectral band at ca. 320 nm at ambient temperature were recorded at a 30 min gap for a period of 12 h. The stability of the compounds in solution at pH 1.2 and 2.1 (50 mM KCl/HCl buffer), 3.1 (50 mM citrate buffer), and 4.4, 7.0, or 8.0 (50 mM phosphate buffer) was measured similarly.

Moreover, the ^{51}V and ^{95} Mo NMR spectra of the pV and pMo compounds were monitored over a period of 12 h for any change in the spectral pattern.

Effect of Catalase on the Complexes. The effect of catalase on complexes was studied by determining the peroxide content of the compounds in a solution containing catalase at specified time intervals. The test solution contained phosphate buffer (50 mM, pH 7.0) and catalase (40 μg/mL). The volume of the reaction solution was kept at 70 mL. The solution was incubated at 30 °C. The polymeric compound was then added to the test solution, and aliquots of 5 mL were pipetted out and titrated for peroxide content after stopping the reaction by adding it to cold sulfuric acid (0.7 M, 100 mL) at an interval of 5 min from the starting of reaction. In order to obtain a measurable rate in the case of the free mononuclear compounds **DMo$_1$** or **DMo$_2$**, the amount of catalase used was 10 μg/mL. Degradation of the compounds with respect to their loss of peroxide was also followed by monitoring the band at ca. 320 nm with time. For the polymer-bound compounds concentrations were on the basis of actual peroxometal loading (mmol g^{-1}).

Measurement of Alkaline Phosphatase Activity. Phosphatase activity was assayed spectrophotometrically by using *p*-NPP as a substrate. The continuous production of *p*-nitrophenol (*p*-NP) was determined at 30 °C by measuring the absorbance at 405 nm in a reaction mixture containing ALP from rabbit intestine (3.3 μg protein/ml), *p*-NPP (2 mM) in incubation buffer (25 mM glycine + 2 mM $MgCl_2$, pH 10.0). The initial reaction rates were obtained by starting the reaction by adding ALP to the reaction solution, which was preincubated for 5 min. The initial reaction rate of *p*-NPP hydrolysis in the absence of the inhibitors, V_0, was determined which was used as control. The effects of pV, pMo, and bare ligands were assessed by adding different concentrations of each species in the ALP assay. For the polymer-bound compounds concentrations were on the basis of actual peroxometal loading (mmol g^{-1}). The IC_{50} values were graphically determined as the half-maximal inhibitory concentration of the inhibitor species giving 50% inhibition. All assays were performed in triplicate. The data in the figures are presented as the means ± SE from three separate experiments.

Determination of Kinetic Parameters. The enzyme kinetic studies were carried out by using Cary 100 Bio Enzyme Kinetics software. The kinetic parameters V_{max} and K_m were determined using a Lineweaver −Burk plot following rearrangement of the Michaelis−Menten equation

$$\frac{1}{V} = \left\{\frac{K_m}{V_{max}[S]} + \frac{1}{V_{max}}\right\}$$

The parameter V_{max} is the maximal velocity, and K_m is the Michaelis constant, its value being equivalent to the substrate concentration at which velocity is equal to one-half of $V_{max}/2$. V_{max} and K_m can be obtained from the intercept and slope, respectively. In the present case, the expression for velocity of the reaction is given by

$$V = \left\{\frac{V_{max} \times [S]}{K_m\left(\frac{1 + [I]}{K_i}\right) + [S]\left(\frac{1 + [I]}{K_{ii}}\right)}\right\}$$

where V is the velocity, [S] is the *p*-NPP concentration, [I] is the inhibitor concentration, K_i is the inhibitory constant for the competitive part, and K_{ii} is the inhibitory constant for the noncompetitive part. The enzyme inhibitor and enzyme substrate inhibitor constants were calculated from secondary plots of initial rate data by linear regression analysis. The slopes obtained from Lineweaver plots were replotted against inhibitor concentration to obtain K_i values from the x intercepts of these replots. The intercepts obtained from Lineweaver plots were replotted against inhibitor concentration to obtain K_{ii} values from the x intercepts of these replots.

RESULTS AND DISCUSSION

Synthesis and Characterization. The degree of dissociation as well as mode and extent of chelation of the water-soluble polyelectrolytes used as support in the present study are known to be strongly dependent on pH.[28] The advantages of using a

Table 1. Analytical Data for the Polymer-Bound Peroxometallates

	% found from elemental analysis (% obtained from EDX spectra)						metal-ion loading[a]
compound	C	H	N	Na	M	O_2^{2-}	(mmol g^{-1} of polymer)
PV_3	29.31 (29.69)	2.87		(17.22)	10.32 (10.62)	12.21	2.02
PV_4	24.61 (24.97)	3.89		(17.01)	8.78 (8.85)	10.73	1.72
PMo_1	30.52 (30.76)	2.34		(19.19)	13.92 (13.88)	9.31	1.45
PMo_2	39.74 (40.07)	4.53		(19.89)	6.50 (6.39)	4.30	0.68
PMo_3	46.72 (46.89)	6.96	17.79 (17.13)		5.82 (5.79)	3.71	0.61

[a] Metal-ion loading = (observed metal% × 10)/(atomic weight of metal).

soluble polymeric ligand for the synthesis of polymer-bound metal complexes include the possibility of adopting synthetic procedures used for preparing their low molecular weight analogues and facility of product characterization due to the homogeneity afforded by the soluble support.[20b] In a solution of vanadate or molybdate and excess H_2O_2 at pH ≥ 5, formation of diperoxo species of these metals is favored.[29] In the present study, the strategically maintained pH of ca. 6 was found to be optimum for the formation of the diperoxovanadate moieties and their coordination to the sulfonate and maleate pendant groups of the polymers PSS and PSSM, respectively, leading to the desired synthesis of the compounds. Employing a somewhat similar synthetic methodology based on the reaction of molybdic acid, H_2MoO_4, with 30% H_2O_2 and the respective polymer at pH ca. 5, compounds **PMo_1**, **PMo_2**, and **PMo_3** were obtained. The other essential components of the synthetic methodology included maintenance of required time and temperature at ≤4 °C (−5 °C for **PV_3**) and limiting water to that contributed by 30% H_2O_2 and alkali hydroxide solution. The alkali used to raise the pH of the reaction solution also served as a source of additional countercation for the complex anions. The compounds were isolated by solvent precipitation, which is an effective and general way of isolating soluble polymers.[20] Our attempts to incorporate pMo moiety to PSS or PSSM chains or to improve the metal loading in the synthesized compounds have not been successful so far. Whereas a reasonably good metal:ligand ratio was obtained for compounds **PV_3** (2:3) and **PV_4** (1:2), the same was found to be rather low for the pMo compounds (1:4 for **PMo_1**, 1:7 for **PMo_2**, and 1:12 for **PMo_3**). In the solid state, the compounds were found to be stable for several weeks stored dry in closed containers at <30 °C. The polymer-anchored compounds are soluble in water.

The elemental analysis data for each of the polymeric compounds **PV_3**, **PV_4**, **PMo_1**, **PMo_2**, and **PMo_3** indicated the presence of two peroxide groups per metal center. The compounds were diamagnetic in nature, as was evident from the magnetic susceptibility measurement in conformity with the presence of V and Mo in their +5 and +6 oxidation states, respectively. The metal loading on the compounds based on elemental analysis and confirmed by EDX analysis are presented in Table 1.

SEM and Energy-Dispersive X-ray (EDX) Analysis. Scanning electron microscopy was employed to study the morphological changes occurring on the surfaces of the polymers after loading of the peroxometallates to the polymer matrices. The micrographs of the polymer-anchored complexes showed significant roughening of their surfaces, in contrast to the smooth surfaces of the pure polymers (Figure 1), and revealed that the metal ions are distributed across the surface of the polymers. Data obtained on the composition of the compounds from energy-dispersive X-ray spectroscopy, which provides in situ chemical analysis of the bulk, were in good agreement with the elemental analysis values (Table 1). EDX analysis was carried out focusing multiple regions over the surface of the polymer. The data presented in Table 1 is the averaging out of the data from these regions.

IR and Electronic Spectral Studies. The significant general features of IR spectra of the polymer-anchored peroxo complexes of V(V) and Mo(VI) are summarized in Table 2. The spectra for complexes **PV_4**, **PMo_1**, **PMo_2**, and **PMo_3** are presented in Figure S1, Supporting Information. The strong absorption at ca. 960 cm^{-1} has been assigned to the ν(M═O) mode of the terminal M═O (M = V or Mo) group.[30] The bands observed due to the metal peroxo moiety of the macrocomplexes were in the range characteristic of side-on-bound peroxo ligand.[29b]

By comparison of IR spectra of the anchored complexes to the spectra of pure polymers and available literature data on metal compounds with a coordination environment comprised of ligands relevant to the present study, fairly reliable empirical assignments could be derived for the characteristic IR bands observed for the title compounds. It has been demonstrated earlier that the $\Delta\nu = \nu_{asym} - \nu_{sym}$ relationship with the carboxylato coordination, derived from thorough investigation on carboxylato complexes having known crystal structures,[31] also holds for polycarboxylates[32] as well as polyacrylates.[33]

Typical for the spectra of pristine polymers PA and PMA as well as metal-anchored compounds **PMo_1** and **PMo_2** are the bands between 1710 and 1540 cm^{-1} attributable to ν_{asym}(COO) and in the range of 1415 and 1406 cm^{-1} due to the ν_{sym}(COO) mode. In free PA, ν_{asym}(COO) and ν_{sym}(COO) modes are observed at 1565 and 1409 cm^{-1}, respectively ($\Delta\nu$ = 156 cm^{-1}). In the spectrum of **PMo_1**, a distinct shift of the ν_{asym}(COO) band to a higher frequency of 1574 cm^{-1} with some broadening was noted, although $\Delta\nu$ (168 cm^{-1}) remained close to that observed for free PA. The observation is characteristic of a bridged bidentate mode of coordination of the carboxylate group.[31,33] The broadening of the band at 1574 cm^{-1} is likely to be due to the presence of uncoordinated carboxylates in the compound. The spectrum of pure PMA displays ν_{asym}(COO) and ν_{sym}(COO) absorptions at 1540 and 1415 cm^{-1}, respectively. In the case of **PMo_2**, ν_{asym}(COO) was observed as a strong

dx.doi.org/10.1021/ic200368g |*Inorg. Chem.* 2011, 50, 8046–8062

broad band at 1659 cm^{-1}. The corresponding $\nu_{sym}(COO)$ mode attributable to coordinated carboxylate group appeared at 1407 cm^{-1} with a shoulder at 1414 cm^{-1}, probably owing to the presence of free carboxylate. The resulting $\Delta\nu$ = 252 cm^{-1} being much greater relative to the free PMA ($\Delta\nu$ = 135 cm^{-1}) gave clear indication of the presence of unidentately coordinated carboxylate groups in the compound. The presence of free COOH groups in each of the compounds $\mathbf{PMo_1}$ and $\mathbf{PMo_2}$ was evident from an additional IR band appearing in the vicinity of 1710 cm^{-1}.

In poly(acrylamide), the pendant amide groups have two potential alternative metal binding sites viz. amide nitrogen or the carbonyl oxygen.[34] Coordination through the lone pair of nitrogen is known to cause an increase in the ν(C═O) (amide I) band frequency, in contrast to bonding via the carbonyl oxygen which shifts the carbonyl absorption to a lower value.[34a−c] The pure PAm has a strong carbonyl stretching absorption at 1643 cm^{-1}, whereas the spectrum of the complex exhibited, in addition to the band at 1643 cm^{-1}, a new characteristic band in the carbonyl region at 1658 cm^{-1}. This later band is attributable to a shift of the amide I absorption to a higher frequency, resulting from coordination of the Mo(VI) ion with the N (amide) atom. ν(C−N) was identified at 1425 cm^{-1} as a medium-intensity band with a shoulder at 1445 cm^{-1}. N−H stretching could not be assigned with certainty as it occurred at a O−H frequency region.

In the spectra of the pure polymers PSS and PSSM, the bands representing S−O stretching of the pendant sulfonate group occur at ca. 1210 and ca. 1130 cm^{-1}, respectively.[34a] The band at ca. 1040 cm^{-1} is due to the symmetric stretching vibration of sulfonate anion.[34f] The spectra of the complexes $\mathbf{PV_3}$ and $\mathbf{PV_4}$ show a distinct splitting pattern displaying bands at 1219 and 1189 cm^{-1} in addition to antisymmetric vibration of S−O at 1127 cm^{-1} that we attribute to complexed sulfonate group.[34a,f,35] Furthermore, the observance of a stretching mode of the sulfonate anion at 1210 cm^{-1} indicates the presence of free sulfonate anion. The spectra of the compounds exhibited characteristic absorptions at ca. 1640 and 1494 cm^{-1} due to its phenyl group and bending CH_2, respectively. For compound $\mathbf{PV_4}$, the spectrum displayed additional bands at 1584 and 1408 cm^{-1} characteristic of the antisymmetric and symmetric stretching modes of carboxylate moieties belonging to the maleate group. Since the $\Delta\nu = \nu_{asym} - \nu_{sym}$ of the carboxylate group obtained from the spectrum of the compound (176 cm^{-1}) is close to that observed for the free polymer (167 cm^{-1}),[31a,33] we infer that the carboxylate group in the PSSM chain, as in $\mathbf{PV_1}$ and $\mathbf{PMo_1}$, coordinates to V(V) in a bidentate bridging fashion. The occurrence of a free −COOH group in the compound was indicated by the absorption at

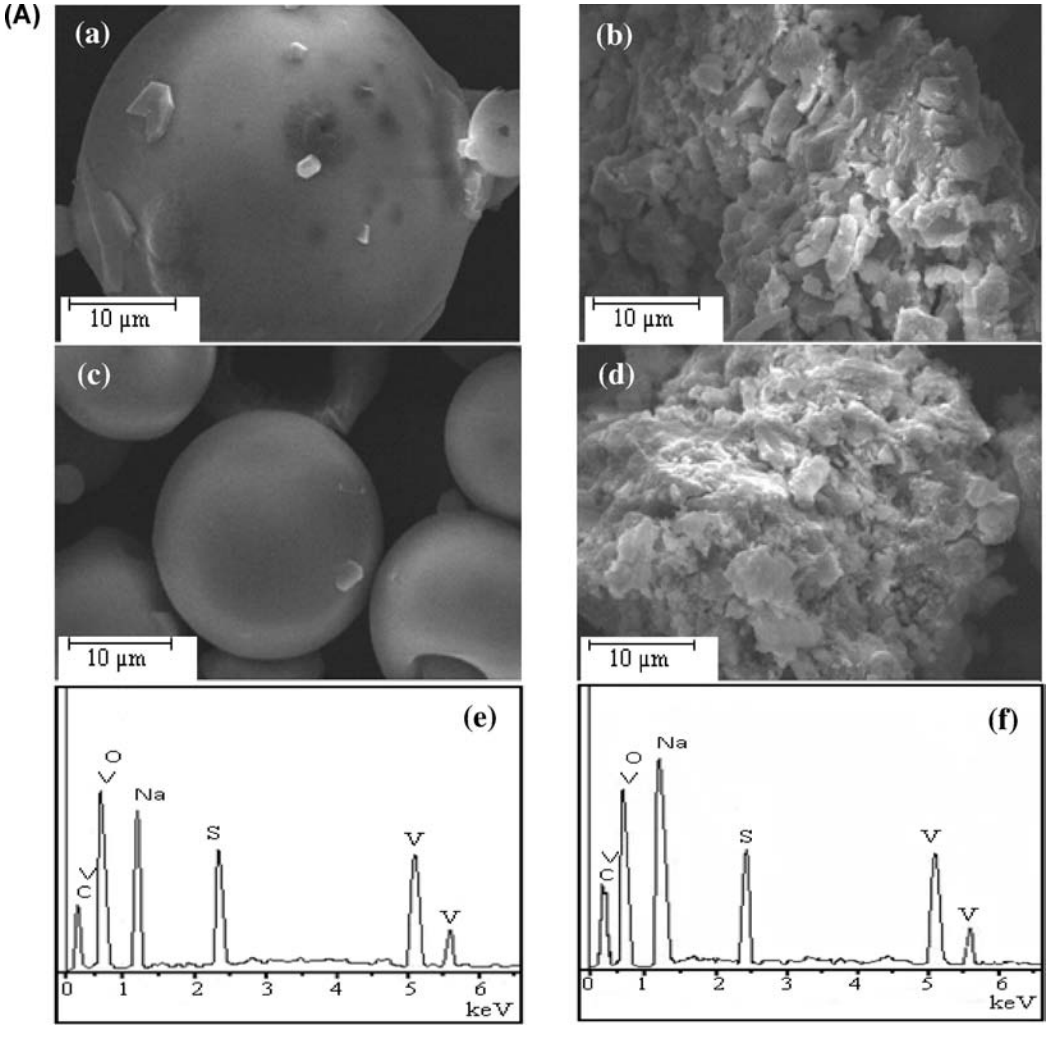

Figure 1. Continued

dx.doi.org/10.1021/ic200368g |*Inorg. Chem.* 2011, 50, 8046–8062

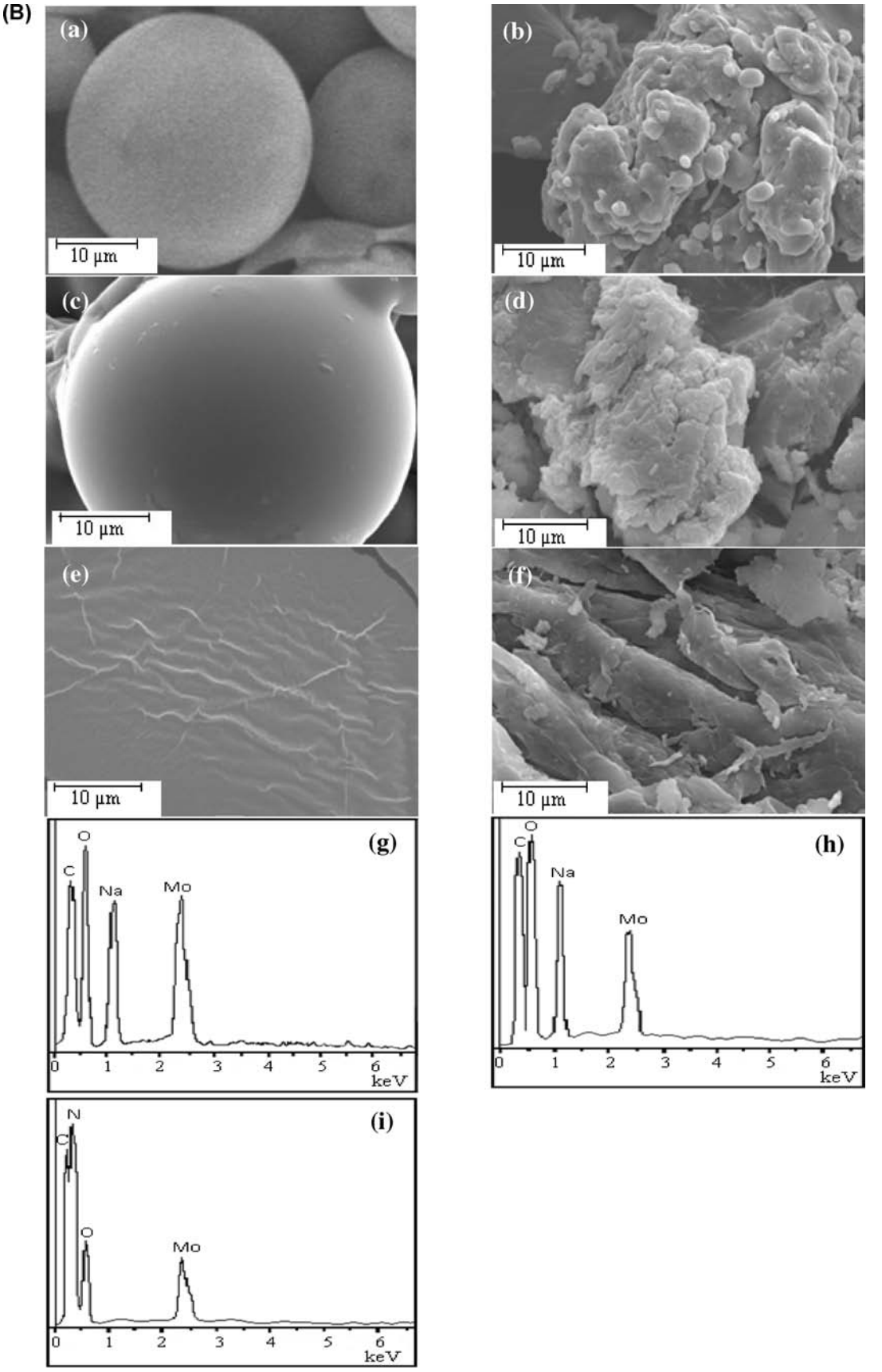

Figure 1. (A) Scanning electron micrographs of (a) PSS, (b) $\mathbf{PV_3}$, (c) PSSM, and (d) $\mathbf{PV_4}$. EDX spectra of (e) $\mathbf{PV_3}$ and (f) $\mathbf{PV_4}$. (B) Scanning electron micrographs of (a) PA, (b) $\mathbf{PMo_1}$, (c) PMA, (d) $\mathbf{PMo_2}$, (e) PAm, and (f) $\mathbf{PMo_3}$. EDX spectra of (g) $\mathbf{PMo_1}$, (h) $\mathbf{PMo_2}$, and (i) $\mathbf{PMo_3}$.

dx.doi.org/10.1021/ic200368g |*Inorg. Chem.* 2011, 50, 8046–8062

Table 2. Infrared Spectral Data for the pV and pMo Compounds[a]

PV_1	PV_2	PV_3	PV_4	PMo_1	PMo_2	PMo_3	Assignment
969(vs)	966(vs)	968(vs)	969(vs)	963(vs)	963(vs)	961(vs)	ν(M=O)
872(vs)	875(vs)	870(vs)	873(vs)	864(vs)	853(vs)	861(vs)	ν(O-O)
525(m)	526(m)	525(m)	530(m)	525(m)	527(m)	509(m)	ν_{sym}(M-O_2)
618(m)	637(m)	618(m)	617(m)	626(m)	610(m)	600(m)	ν_{asym}(M-O_2)
1712(s)	1711(s)		1710(s)	1710(s)	1708(s)		ν_{asym}(COO)
1573(br,s)	1660(br,s)		1584(br, s)	1574(br, s)	1659(br, s)		
1406(s)	1406(s)		1408(s)	1406(s)	1407(s)		ν_{sym}(COO)
		1218(vs)	1219(vs)				
		1188(vs)	1189(vs)				
		1210(sh)	1210(sh)				ν(S-O)
		1129(vs)	1127(vs)				
		1040(s)	1040(s)				
						1643(sh)	ν(C=O)
						1658(br, s)	
						1425(m)	ν(C=N)

[a] vs, very strong; br, broad; s, strong; sh, shoulder; m, medium.

Table 3. Thermogravimetric Data for pV and pMo Compounds

compound	temperature range (°C)	observed weight loss (%)	final residue (%)
PV_3	69−110	2.61	44.37
	110−242	11.80	
	412−600	41.22	
PV_4	68−107	2.06	49.62
	107−206	10.64	
	290−650	37.68	
PMo_1	68−90	3.36	46.01
	90−227	9.34	
	312−591	41.29	
PMo_2	63−101	2.12	50.34
	107−188	4.10	
	313−553	43.44	
PMo_3	69−105	1.07	26.83
	145−184	3.45	
	211−333	18.38	
	333−447	50.27	

1710 cm^{-1}. The IR spectrum of PV_4 thus provided evidence for the involvement of both sulfonate and carboxylate groups of the copolymer in formation of vanadium−polymer linkages.

Weak bands observed in the far-IR region between 500 and 400 cm^{-1} in the spectra of each of the pV and pMo compounds have been assigned to metal oxygen vibrations. The occurrence of lattice water in the title complexes was apparent from the appearance of strong and broad ν(OH) absorptions displayed at 3500−3400 cm^{-1}.

The electronic spectrum of each of the pV as well as pMo compounds recorded in aqueous solution displayed a weak-intensity broad band at 310−330 nm which was assigned to a peroxo to metal (LMCT) transition. The band was observed in the range characteristic of a diperoxo species of vanadium(V) or molybdenum(VI).[15a,24]

TGA-DTG Analysis. The thermogravimetric analysis data revealed that the polymer-anchored peroxo compounds undergo multistage decomposition after initial dehydration (Table 3). It is notable that the complexes, unlike some monomeric peroxomolybdenum compounds,[36] do not explode on heating. The TG-DTG plots for compounds PV_4 and PMo_3 are presented in Figure S2, Supporting Information. The first stage of decomposition occurring in the temperature range of ca. 70−110 °C for each of the pV and pMo compounds correspond to liberation of molecules of water of crystallization from the complexes. The second decomposition stage is in the temperature range of 108−250 °C attributable to complete loss of coordinated peroxo groups from the complexes. The absence of peroxide in the decomposition product, isolated at this stage, was confirmed from IR spectral analysis. The loss of peroxide is seen to be followed by a two-stage decomposition in the range 412−600 °C for PV_3 possibly due to loss of the sulfonate group and rupturing of polymers, whereas three-stage decomposition occurs in the broad temperature range of 290−650 °C for PV_4 which may be ascribed to decarboxylation and loss of sulfonate functionals accompanied by break up of the polymer matrix. Further evidence regarding decarboxylation and desulfonation of the polymers was obtained from the IR spectra recorded after heating the compounds separately up to the final decomposition temperature, which showed complete disappearance of the strong peaks originating from ν_{asym}(COO), and bands due to S−O stretching of the spectra of the original compounds.

In the case of the pMo compounds, the decomposition stage associated with decarboxylation and breakdown of the polymer was observed in the temperature ranges of 312−591 °C (PMo_1) and 313−553 °C (PMo_2), respectively. The compound PMo_3 on heating to a temperature of 750 °C, after loss of peroxo groups, undergoes final decomposition consisting of two weight-loss processes in the temperature range of ca. 211−447 °C due to breakdown of the polymer ligand (Figure S2, Supporting

dx.doi.org/10.1021/ic200368g |*Inorg. Chem.* 2011, 50, 8046–8062

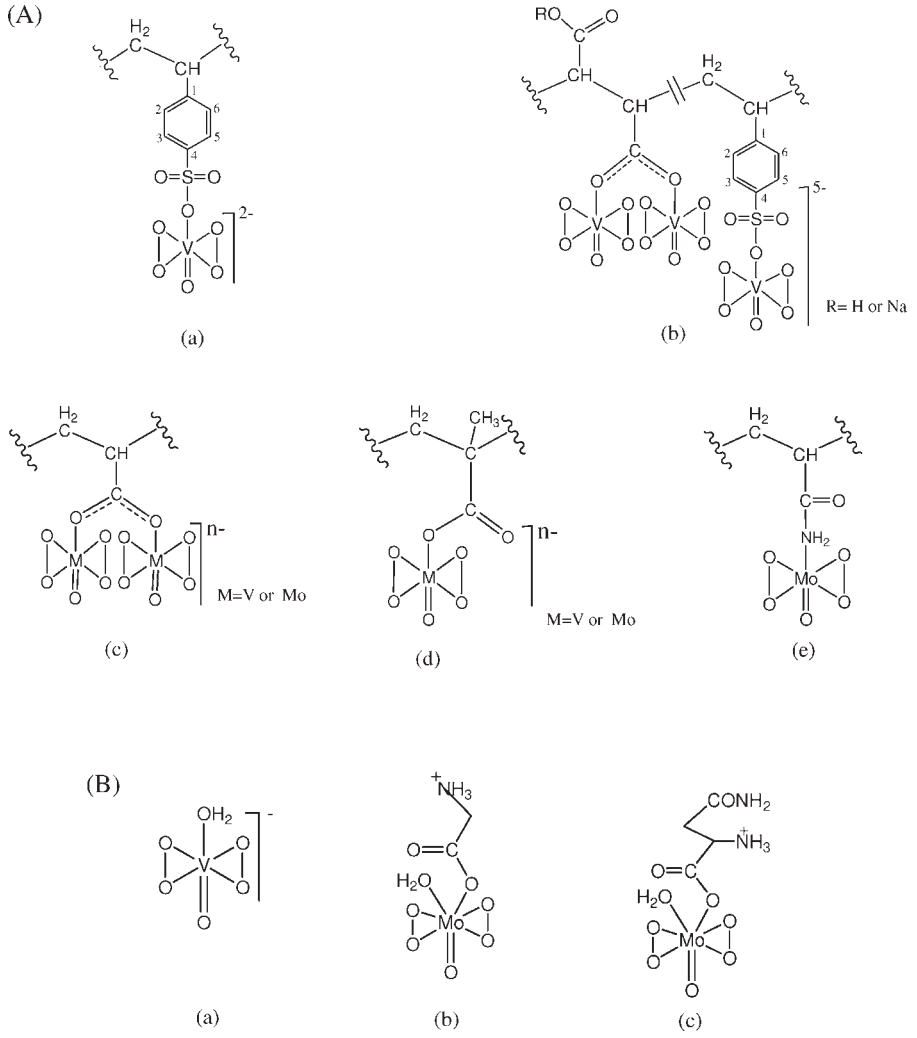

Figure 2. Peroxo compound of vanadium(V) and molybdenum(VI) under investigation in the current study. (A) Proposed structures of polymer-anchored compounds: (a) $\mathbf{PV_3}$, (b) $\mathbf{PV_4}$, (c) $\mathbf{PV_1}$ ($n = 3$) and $\mathbf{PMo_1}$ ($n = 1$), (d) $\mathbf{PV_2}$ ($n = 2$) and $\mathbf{PMo_2}$ ($n = 1$), and (e) $\mathbf{PMo_3}$. Wavy line represents polymer chain. (B) Structures of (a) **DPV**, (b) $\mathbf{DMo_1}$,[24] and (c) $\mathbf{DMo_2}$.[24]

Information). By analogy with the thermal decomposition characteristics reported for some polyacrylamides,[37] we attribute the first stage of decomposition (211−333 °C) to release of water, ammonia, and a small amount of carbon dioxide from the pendant amide groups where the polymer chains remain intact.[37] In the second stage of decomposition (333−447 °C) main chain breakdown occurs accompanied by a majority of weight loss (50.27%).

The sticky residue from the pMo compounds, after complete loss of the components viz. lattice water, coordinated peroxide and polymeric functionals, was found to be a hydrated oxomolybdenum species. This was evident from the IR spectra which displayed the characteristic ν(Mo═O) and ν(OH) absorptions and was devoid of bands attributable to peroxo and the polymeric ligands of the original compound. The residue obtained from the pV compounds was similarly characterized to be oxo species of vanadium. Thermogravimetric analysis data of the compounds thus provided further evidence in support of their composition and formula assigned.

On the basis of the above data, a structure of the type shown in Figure 2A(a), has been envisaged for the polymer-anchored pV complex, $\mathbf{PV_3}$. The proposed structure for complex $\mathbf{PV_4}$ that includes V atoms coordinated to the polymer chain via the bridged carboxylate of maleate group, unidentate sulfonate group, side-on-bound peroxo, and terminal V═O is shown in Figure 2A(b). The results are also consistent with the proposed structures of the pMo-containing macrocomplexes $\mathbf{PMo_1}$, $\mathbf{PMo_2}$, and $\mathbf{PMo_3}$ presented in Figure 2A(c−e).

The absence of an additional bridging ligand in the dinuclear peroxometal species of compounds $\mathbf{PV_1}$, $\mathbf{PV_4}$, and $\mathbf{PMo_1}$ may appear unusual in the context of existing reports on dimeric pV and pMo compounds.[8c,15b,15c,29b,38] A carboxylate bridge in such compounds is usually accompanied by an additional bridge formed by ligands such as aquo, μ-oxo, or μ-peroxo.[8c,15b,15c,38i−38l] The reports available so far are however limited to the structures of free or unsupported dinuclear peroxometal complexes. It is reasonable to expect that in the polymer-anchored complexes the interchain interaction between the dinuclear peroxometal centers and the neighboring pendant carboxylate groups of the polymer chains would provide additional support to the carboxylate-bridged diperoxo metal moieties.

^{13}C NMR Studies. Crucial information regarding the bonding pattern of the macromolecular ligands to the metal centers in the

dx.doi.org/10.1021/ic200368g |*Inorg. Chem.* 2011, 50, 8046–8062

Table 4. ^{13}C NMR Chemical Shift for Polymer-Anchored pV and pMo Compounds and Base Polymers

	chemical shift (ppm)										
	carboxylate/amide carbon					ring carbon					
compound	free	complexed	CH	CH_2	CH_3	C1	C2	C3	C4	C5	C6
PA	184.50		45.52	36.10							
PV_1	184.33	215.45	45.42	36.14							
PMo_1	184.51	215.51	45.81	36.04							
PMA	187.41		46.01	17.36	56.54						
PV_2	187.63	215.37	45.96	17.22	56.40						
PMo_2	187.53	215.47	46.78	17.32	56.42						
PAm	179.49		41.66	34.88							
PMo_3	179.48	200.13	41.66	34.91							
PSS			40.52	44.14		140.35	128.84	125.57	148.55	125.35	128.17
PV_3			40.63	44.57		140.28	128.37	125.51	148.69	125.51	128.06
PSSM	179.95		57.79[a]	30.02		140.51	128.61	125.67	145.68	125.56	128.61
	180.46		44.99[b]								
			36.87[c]								
PV_4	179.78	211.22	57.03[a]	31.10		140.67	128.82	125.68	145.13	125.18	128.34
	180.21		44.91[b]								
			36.93[c]								

[a] CH group of the maleate moiety attached to the CH group of the styrene sulfonate moiety. [b] CH group of the styrene sulfonate moiety. [c] CH group of the maleate moiety attached to the CH_2 group of the styrene sulfonate moiety.

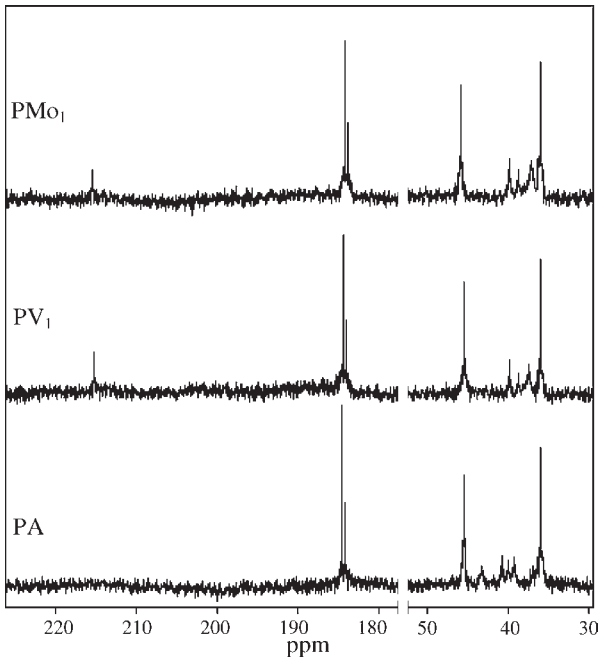

Figure 3. ^{13}C NMR spectra of PA, **PV_1**, and **PMo_1** in D_2O.

compounds and their stability in solution was provided by ^{13}C NMR data. The study of coordination-induced ^{13}C NMR chemical shifts has been recognized as an important tool in understanding the mode of coordination of the heteroligands in peroxo metal compounds.[36,38i,39] ^{13}C NMR data pertaining to the polymer-bound compounds as well as the pure polymers are presented in Table 4. The major peaks were interpreted on the basis of available literature data.[36,38i,39,40] The ^{13}C NMR spectra of pristine polymers PA and PMA display, in addition to the characteristic signals corresponding to chain carbon atoms, resonances due to the carboxylate carbon atoms centered at 184 and 187 ppm, respectively[40] (Figure 3 and Table 4). Two closely spaced peaks observed in this region are likely to be due to the presence of free carboxylate as well as −COOH groups of the polymers in solution. A striking common feature observed in the spectra of each of the polymeric compounds after metal anchoring via the carboxylate group (**PV_1**, **PV_2**, **PMo_1**, and **PMo_2**) is the appearance of a new peak at a considerably lower field of ca. 215 ppm attributable to the carbon atom of the complexed carboxylate group. The substantial downfield shift, $\Delta\delta$ ($\delta_{complex} - \delta_{free\ carboxylate}$) $\approx$ 31 ppm in the case of PA-bound compounds and ca. 27 ppm in the metal-anchored PMA compounds relative to the free carboxylate peak of the pristine polymer suggests strong metal ligand interaction. It is notable that for compounds **PV_1** and **PMo_1**, with the bridging carboxylate coordination to the V(V) or Mo(VI), the observed downfield shift of the peak due to complexed carboxylate is consistently higher ($\Delta\delta \approx 31$ ppm) than the ones (**PV_2** and **PMo_2**) with monodentate carboxylate coordination ($\Delta\delta \approx 27$ ppm). The resonance occurring as a singlet in each case evidenced for a single carbon environment for complexed carboxylates, obviously resulting from a single mode of metal carboxylate coordination, in agreement with the proposed structures.

The ^{13}C NMR spectrum of PAm in solution has been thoroughly investigated by others under varying pH conditions.[41] The spectrum of the pMo-incorporated poly(acrylamide) compound, **PMo_3**, provided evidence for the presence of complexed as well as free amide groups by displaying a new peak at 200.13 ppm, in addition to the characteristic amide resonance at 179.48 ppm corresponding to the free amide groups as observed in the pure polymer (Table 4).

In the spectra of compounds **PV_3** as well as **PV_4**, peaks due to poly(sodium styrene sulfonate) matrix remained practically

dx.doi.org/10.1021/ic200368g |*Inorg. Chem.* 2011, 50, 8046–8062

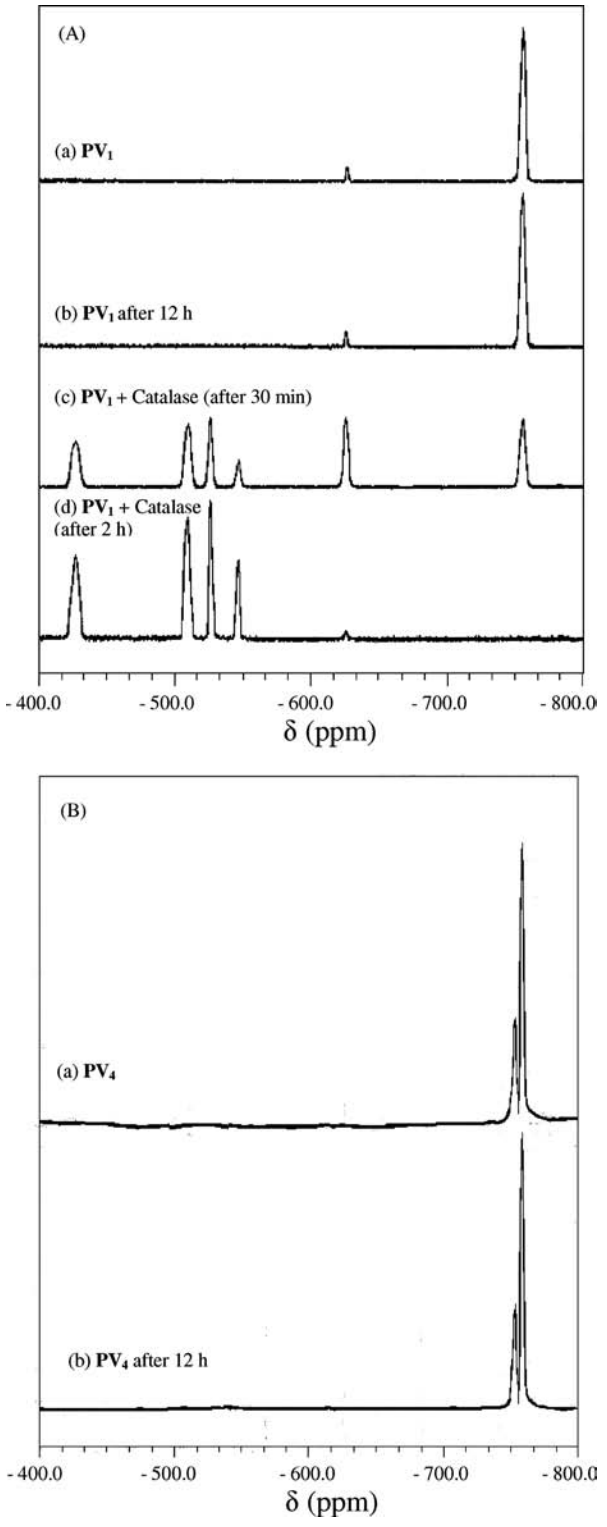

Figure 4. (A) ^{51}V NMR spectra of a 0.2 mM solution of $\mathbf{PV_1}$, its catalase degradation products. The spectra were recorded as follows: (a) aqueous solution of $\mathbf{PV_1}$ in water immediately after preparation, (b) solution of (a) 12 h later, (c) $\mathbf{PV_1}$ (0.2 mM) incubated with catalase (40 μg/mL) at 30 °C in phosphate buffer (50 mM, pH = 7) after 30 min, (d) solution of (c) 2 h later. (B) ^{51}V NMR spectra of 0.2 mM solution of $\mathbf{PV_4}$. The spectra were recorded as follows: (a) aqueous solution of $\mathbf{PV_4}$ in water immediately after preparation and (b) solution of (a) 12 h later.

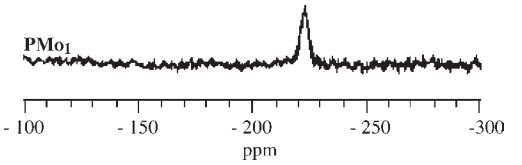

Figure 5. ^{95}Mo NMR spectra of aqueous solution of $\mathbf{PMo_1}$ (2 M).

unaffected by complexation as compared to the pure polymer. This is not unexpected keeping in view that V(V) atoms are bound to the polymer through the sulfonate groups and hence are well separated from the chain as well as ring carbon atoms of the polymer support. The spectrum of the compound $\mathbf{PV_4}$ however, like the other complexes containing carboxylate functional groups, displayed a new peak at 211.22 ppm in addition to the carboxylate resonance corresponding to the free maleate group (180.21 ppm), suggesting the presence of coordinated maleate groups in the compounds. The observed downfield shift of the complexed carboxylate carbon with respect to the free carboxylate was comparable to the poly(sodium acrylate)-bound compounds ($\Delta\delta \approx 31$ ppm), which may be considered as an indication of the similarity in the bonding pattern of the carboxylate groups in the two types of compounds. The findings from the ^{13}C NMR spectral analysis of the compounds under investigation are consistent with the occurrence of retention of their solid-state structure in solution.

^{51}V NMR and ^{95}Mo NMR Studies. Further information regarding the nature and stability of the peroxovanadium as well as peroxomolybdenum-anchored macrocomplexes in solution was derived from ^{51}V NMR and ^{95}Mo NMR studies. On dissolution in water, the ^{51}V NMR spectra of the compounds $\mathbf{PV_1}$, $\mathbf{PV_3}$, and $\mathbf{PV_4}$ displayed major peaks between $\delta = -753$ and -758 ppm. These chemical shifts are within the range commonly observed for diperoxovanadium complexes in various donor ligand environments.[8,17d,42] The spectra of $\mathbf{PV_1}$ and $\mathbf{PV_4}$ are presented in Figure 4. In the spectrum of compound $\mathbf{PV_1}$ a single major signal was found at -757 ppm, which may be assigned to the polymer-bound dinuclear peroxovanadium species (Figure 4A).[42e] In this context, it is significant to note that a ^{51}V NMR signal observed in the spectrum of a solution of vanadate and peroxide at pH 5.5 -7.5 was assigned to a dinuclear tetraperoxovanadate species by Howarth and Hunt.[42e] An additional weak intensity peak observed at -621 ppm indicated the presence of traces of monoperoxovanadate species,[42a] possibly formed due to elimination of a peroxo group from some of the diperoxo moieties. Compound $\mathbf{PV_4}$ showed two closely spaced peaks at -753 and -758 ppm (Figure 4B). These likely refer to complexation of the metal centers through two types of pendent ligand sites viz. sulfonate and maleate carboxylate groups, available on the copolymer matrix, PSSM. In the case of compound $\mathbf{PV_3}$ the major peak was observed at -754 ppm, which may be attributed to the pV moiety bonded to the sulfonate group. The spectrum of the compound $\mathbf{PV_2}$ displayed an intense resonance at -722 ppm, which is in the region characteristic of diperoxovanadate species containing a heteroligand with a carboxylate group bonded to V(V) in a monodentate fashion.[2c,17d,42f] Spectra of compounds $\mathbf{PV_2}$ and $\mathbf{PV_3}$ also showed the presence of traces of monoperoxovanadate by displaying weak intensity peak at -621 ($\mathbf{PV_2}$) and -624 ppm ($\mathbf{PV_3}$).

The ^{95}Mo NMR technique has been used as a sensitive and useful tool for study of the structure of molybdenum peroxo

dx.doi.org/10.1021/ic200368g |*Inorg. Chem.* 2011, 50, 8046–8062

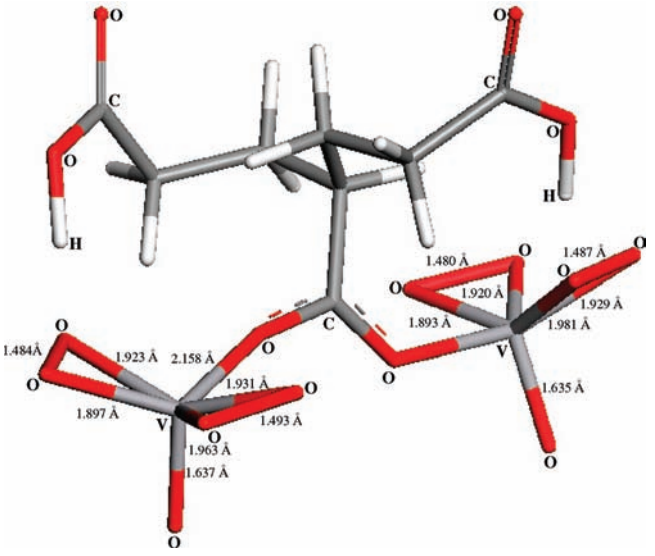

Figure 6. Optimized structure of $\mathbf{PV_1}$ model complex obtained by using BLYP functional and DNP basis set. Selected geometric parameters are also shown in the figure.

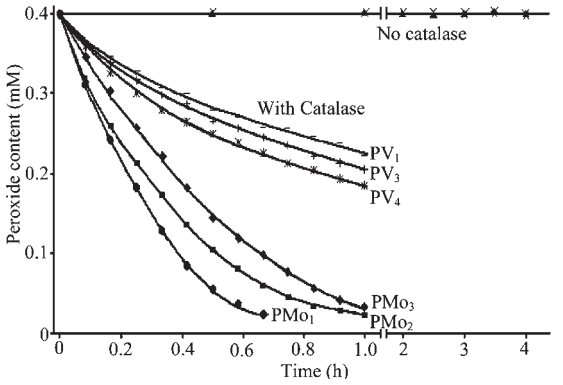

Figure 7. Stability of compound $\mathbf{PV_3}$ at different pH values: (×) compound solution in distilled water, pH of the solution = 6.0, (▲) solution of complexes in phosphate buffer (50 mM, pH 7.0). Effect of catalase on $\mathbf{PV_1}$ (—), $\mathbf{PV_3}$ (+), $\mathbf{PV_4}$ (*), $\mathbf{PMo_1}$ (●), $\mathbf{PMo_2}$ (■), and $\mathbf{PMo_3}$ (♦). The test solution contained phosphate buffer (50 mM, pH 7.0) and the catalase (40 μg/mL) which was incubated at 30 °C for 5 min. Compounds were then added to the reaction solution, aliquots were drawn at indicated time points, and loss in peroxide content was determined. For polymeric compounds concentrations are on the basis of peroxometal loading.

complexes in aqueous solution.[43] The ^{95}Mo NMR spectrum of $\mathbf{PMo_1}$ (Figure 5) displayed a single resonance at −225 ppm (relative to $[MoO_4]^{2-}$), indicating the presence of peroxomolybdenum species.[39a,43] For complexes $\mathbf{PMo_2}$ and $\mathbf{PMo_3}$ similarly only one peak was observed in each of the spectra at δ −217 and −220 ppm, respectively. The appearance of a lone characteristic peak in the ^{95} Mo NMR spectra of the compounds under investigation confirmed the presence of a single coordination environment for the peroxomolybdenum species present in solution.

Density Functional Studies. It is interesting to note that the carboxylate functional group present in the two closely related polymer matrices, poly(acrylate) and poly(methacrylate), binds the pV or pMo moieties in two different coordination modes leading to formation of two structural forms viz. a dimeric tetraperoxometallate ($\mathbf{PV_1}$ and $\mathbf{PMo_1}$) and monomeric diperoxometallate ($\mathbf{PV_2}$ and $\mathbf{PMo_2}$). Such variation in mode of coordination of carboxylate groups present in poly(acrylate) based polymers is not unprecedented.[33] Earlier we proposed that the difference in coordination pattern in the compounds is likely to be a consequence of the presence of $-CH_3$ groups attached to the polymer backbone in PMA which being relatively bulkier probably prevent formation of a dinuclear pV species through a carboxylate bridge.[16]

In order to gain better insight into the aforementioned aspect we carried out a theoretical investigation on the structural and electronic properties of the polymer-supported pV compounds employing the density functional theory (DFT) method. A model complex has been generated corresponding to a section of the pV-anchored complex $\mathbf{PV_1}$, containing three repeating units of the polymer with one dinuclear pV moiety bound through a bridging carboxylate group (Figure 6). DFT calculations were performed on this model complex using the BLYP functional and DNP basis set as implemented in the program DMol^3.[44] The complex was first optimized at the BLYP/DNP level, and then vibrational frequencies were calculated at an optimized structure to conform to the stability of the complex. In the vibrational frequency calculations, no imaginary frequency was found for the model complex, suggesting that the complex represents a stable structure. The selected geometrical parameters obtained for the complex are in good agreement with available experimental data.[17f] Calculations were performed similarly on a complex generated by replacing the α-hydrogen of the repeating unit by a methyl group so as to model the compound attached to a PMA chain. A negative vibrational frequency (imaginary frequency) was obtained in this case. The appearance of an imaginary frequency in the vibrational frequency calculations indicates that this structure is an unstable one on the potential energy surface. We further calculated the chemical softness values for both model complexes from their HOMO and LUMO energies. The chemical softness values of hydrogen and methyl-substituted complexes are 24.755 and 26.464 au^{-1}, respectively. The higher softness value obtained for the later model complex indicated the lower stability of the complex compared to the α-hydrogen containing one.

Similar experiments were performed on model complexes containing monomeric pV moieties. It is notable that the presence of monomeric pV units, bonded through a monodentate carboxylate, in the model complex corresponding to $\mathbf{PV_2}$ afforded a stable structure. In the case of PA-supported complex, model complexes with monomeric pV units provided a structure of comparable stability with the one containing a dimeric pV unit. The results are consistent with the proposed structures for complexes $\mathbf{PV_1}$ and $\mathbf{PV_2}$ [Figure 2A(c,d)].

Stability of the Compounds Toward Decomposition in Solution. The stability of each of the title compounds $\mathbf{PV_3}$, $\mathbf{PV_4}$ and $\mathbf{PMo_1}$, $\mathbf{PMo_2}$, $\mathbf{PMo_3}$ with respect to the loss of peroxide in solution at pH ca. 6.0, the natural pH attained by the solution on dissolving the compounds, has been examined by determining their peroxide content and monitoring the absorbance at 310−330 nm region in the electronic spectra at specified time intervals for any possible change. Similarly, the stability of the mononuclear complexes, $\mathbf{DMo_1}$ and $\mathbf{DMo_2}$, was investigated in solution of their respective natural pH values, viz. pH 1.5 ($\mathbf{DMo_1}$) and 3 ($\mathbf{DMo_2}$). The studies revealed that the peroxide content of the compounds tested and the position and intensity

dx.doi.org/10.1021/ic200368g |Inorg. Chem. 2011, 50, 8046–8062

Table 5. Catalase-Dependent Oxygen Release from Peroxometallates

compound	concentration (mg/mL)	peroxide content (mM)	loss of peroxide (μM/min)
$\mathbf{PV_1}$[a]	0.110	0.4	5.80
$\mathbf{PV_2}$[a]	0.140	0.4	5.60
$\mathbf{PV_3}$	0.099	0.4	6.51
$\mathbf{PV_4}$	0.116	0.4	7.07
$\mathbf{PMo_1}$	0.137	0.4	17.81
$\mathbf{PMo_2}$	0.294	0.4	17.57
$\mathbf{PMo_3}$	0.327	0.4	10.34
DPV	0.034	0.4	12.00
$\mathbf{DMo_1}$[b]	0.054	0.4	37.60
$\mathbf{DMo_2}$[b]	0.065	0.4	28.33

[a] Reference 16. [b] Amount of catalase = 10 μg/mL.

of their electronic spectral bands remained unaltered even after a period of over 12 h. Figure 7 shows that the compound $\mathbf{PV_3}$, used as a representative, is stable in a solution of pH 5 as well as pH 7. The stability of compounds $\mathbf{PV_1}$ and $\mathbf{PV_2}$ in solution was confirmed and reported previously.[16] We further examined and ascertained the stability of each of the pV and pMo compounds in solutions of pH values ranging from 1.2 to 3.1, 4.4, and 8.0.

It is noteworthy that the ^{51}V and ^{95} Mo NMR spectra of the pV and pMo compounds when monitored over a period of 12 h displayed no change in the spectral pattern (Figure 4). Most importantly, the spectra remained unaltered in solution of a wide range of pH values of 1.2, 3.1, to 8.0 over a period of 12 h. The above results clearly attest to the stability of the compounds in solution.

Thus, all the evidence gathered so far, including the information derived from ^{13}C, ^{51}V, and ^{95} Mo NMR spectral studies, strongly suggest that the compounds under investigation retain their structural integrity in solution. This property of the compounds may also be significant in view of the observation made by Shisheva et al. that orally administered pV was ineffective in inducing normoglycemia in STZ-rats probably because it could not survive the strong acidity of the stomach.[45] Although the observed stability of the compounds in the present study may not imply their stability in vivo, yet it certainly meets one of the criteria for metal complexes to be useful as therapeutic agents.

Effect of Catalase on the Compounds. Catalase is a powerful reactive oxygen (ROS) mopping enzyme responsible for breakdown of H_2O_2 to H_2O and O_2. Since the primary objective of our work has been to explore some of the biochemically relevant properties of the complexes, we considered it important to examine the fate of the compounds in the presence of catalase vis-a-vis H_2O_2, its natural substrate. H_2O_2 is a significant cellular oxidant needed particularly for action of peroxidases that yield highly active intermediates.[4] In the last two decades, the importance of H_2O_2 is increasingly realized as a key signal transducing agent regulating a variety of cellular processes.[3e,f,4,46] Fast decomposition of extracellular H_2O_2 is a constraint for studying the signaling activities of H_2O_2 because cells are equipped with catalase and glutathione peroxidase that rapidly deplete H_2O_2.[3e,f,4] Most experiments on cellular effects of H_2O_2 reported in the literature used concentrations >100 μM in the medium, never known to occur in cells. In order to investigate how the small concentrations of H_2O_2 generated in cells will function in the presence of abundant catalase, it is desirable to have peroxide derivatives easily formed and stable to degradation yet efficient in their action that can substitute for H_2O_2.

It is known that the peroxo group in DPV compared to H_2O_2 is less accessible to degradation by catalase and is active as a substrate in horseradish peroxidase reaction in the presence of catalase at 1/100 concentration.[47] Implicit in these findings is that complexing with vanadium increases the stability of peroxide at the same time they appear to become more efficient in the form of DPV. The feature of common actions of H_2O_2, vanadate, and DPV exemplified as insulin mimics deserve mention.[48] All these three species can enhance protein tyrosine kinase[48] and decrease protein tyrosine phosphatase activities, among other parameters.[1b,c,48] This is possible if they use the same pathway in their actions and signaling. Multiple potential targets are identified for ROS in insulin action,[46] obviously oxidative in nature. Previous studies demonstrated that diperoxovanadate compound can be used as a tool in the study of the signaling actions of H_2O_2.[4,49] In this context, it is noteworthy that some of the heteroligand mononuclear and dinuclear pV and pW complexes synthesized and reported previously by us showed reasonable resistance to catalase action.[18a,c−e] However, no reports seem to be available on the interaction of catalase with discrete pMo compounds in solution.

In the present study, the action of catalase on the newly synthesized compounds was observed to be a slow process in contrast to H_2O_2. Under the effect of catalase the rate of degradation of H_2O_2 with the release of oxygen was reported to be 430 μM/min from a solution of 0.1 mM concentration.[49] As shown by the data presented in Table 5, the synthesized polymer-anchored peroxo complexes are at least 70−100 times weaker as substrates to catalase compared to H_2O_2.

The tested compounds could be arranged in the following order of increasing stability toward degradation under the effect of catalase: $\mathbf{PV_1} \approx \mathbf{PV_2} > \mathbf{PV_3} > \mathbf{PV_4} > \mathbf{PMo_3} > \mathbf{DPV} > \mathbf{PMo_1} \approx \mathbf{PMo_2} \gg \mathbf{DMo_2} > \mathbf{DMo_1}$. From the observed trend, it may be inferred that anchoring of pV or pMo species to a polymer chain enhances, albeit to different extents, the ability of the coordinated peroxo groups of these compounds to resist the action of catalase. The rates of degradation of the polymer-bound diperoxovanadates $\mathbf{PV_3}$ and $\mathbf{PV_4}$ (Table 5) were found to be comparable to that of the previously reported diperoxo compounds of vanadium anchored to soluble polymer, $\mathbf{PV_1}$ and $\mathbf{PV_2}$.[16] These rates are noted to be approximately one-half of that observed for free diperoxovanadate (**DPV**) (12.0 μM/min from a solution of 0.2 mM) under similar reaction conditions.[49] Significantly, however, unlike free **DPV** or some of the heteroligand complexes of vanadium tested previously,[18a,e] monomeric pMo complexes $\mathbf{DMo_1}$ and $\mathbf{DMo_2}$ were observed to undergo rapid degradation, with loss of peroxide within approximately 5 min of incubation. The findings suggest that in the case of the anchored compounds peroxo groups bonded to V(V) are 2−3 orders of magnitude more stable to catalase action than the molybdenum-bound peroxides. The marked influence of the macroligands on the ability of the peroxo metal moiety to withstand catalase action appears to be a consequence of additional stability imparted to the compounds by the polymeric support through immobilization.

We further investigated the nature of the species formed during and after interaction of the pV compounds with catalase using ^{51}V NMR spectra. Degradation of free **DPV** by catalase has been studied and reported previously.[49] Presented in Figure 4A are the spectral changes taking place on incubation of $\mathbf{PV_1}$ with

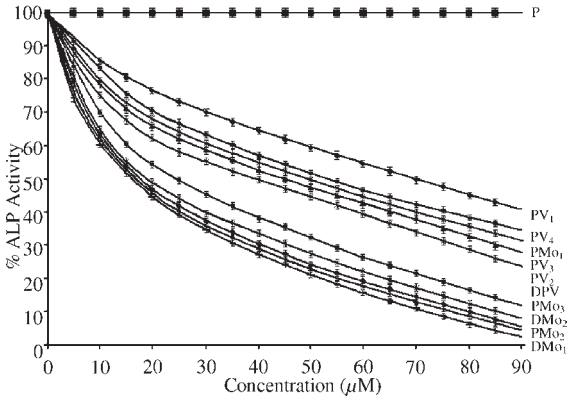

Figure 8. Effect of compounds **PV_1**, **PV_2**, **PV_3**, **PV_4**, **DPV**, **PMo_1**, **PMo_2**, **PMo_3**, **DMo_1**, and **DMo_2** and free polymers (**P**) on the activity of ALP from rabbit intestine. ALP-catalyzed rates of hydrolysis of *p*-NPP at pH 10.0 were determined at 30 °C by measuring A_{405} in a reaction mixture containing ALP (3.3 μg/mL); *p*-NPP (2 mM) in incubation buffer (25 mM glycine + 2 mM $MgCl_2$, pH 10.0) in the absence or presence of stated concentrations of inhibitors. Effects of the additions are represented as the percent values (rounded to integers) of control (Δ*p*-NPP = 3.13 μM/min). Data are presented as means ± SE from three separate experiments. For polymeric compounds concentrations are on the basis of peroxometal loading.

catalase. The spectrum recorded after 30 min of treatment with catalase showed the decrease in intensity of the major peak at −757 ppm with concomitant increase in the intensity of the peak at −621 ppm ascribed to MPV. Additional peaks appeared at −427, −509, and −527 ppm indicating formation of decavanadate (V_{10}) and V_1 (−545 ppm). Monomeric vanadate is known to oligomerize at the concentration and pH used. The small variations from the reported chemical shifts in some cases are likely to be due to variation in pH. The spectrum recorded after 120 min of reaction showed the presence of vanadates as major products with a trace of MPV still remaining in solution. The degradation of the polymer-anchored diperoxovanadate complexes under the effect of catalase leads ultimately to formation of vanadate oligomers via formation of monoperoxovanadate (MPV) intermediate was thus confirmed.

Effect of the Compounds on Alkaline Phosphatase Activity. The effect of different concentrations of polymer-incorporated as well as free mononuclear pV and pMo compounds upon activity of rabbit intestine alkaline phosphatase was investigated using *p*-NPP as substrate and employing an established enzyme assay system. The dose-dependent effects of each of the pV compounds in comparison to the free ligands are presented in Figure 8. To quantify the inhibitory potential of the molecules, we determined the half-maximal inhibitory concentration (IC_{50}) for each inhibitor, which gave rise to a 50% suppression of the original enzyme activity (Table 6). From the data obtained we find that each of the tested species, irrespective of being free or polymer bound, behaved as an active inhibitor of ALP. On comparing the IC_{50} values of the polymeric compounds, in terms of their actual peroxometal loading, with those of free compounds the inhibitors could be arranged in the following order of potency: **DPV** > **PV_2** > **PV_3** > **PV_4** > **PV_1**. In the case of pMo compounds the following trend has been observed: **DMo_1** > **PMo_2** > **DMo_2** > **PMo_3** > **PMo_1**. The pMo compounds were observed to induce stronger inhibition compared to the corresponding vanadium-containing analogue. The effect of each of

Table 6. Half-Maximal Inhibitory Concentration (IC_{50}) and Inhibitor Constants (K_i and K_{ii}) Values for pV and pMo Compounds and Other Inhibitors Against ALP[a]

inhibitor	IC_{50} (μM)	K_i (μM)	K_{ii} (μM)	K_{ii}/K_i	type of inhibition
PV_1	72.45	71.42	70.38	0.99	noncompetitive
PV_2	41.34	49.29	48.50	0.98	noncompetitive
PV_3	45.25	54.50	53.80	0.98	noncompetitive
PV_4	52.54	59.98	59.71	0.99	noncompetitive
PMo_1	48.64	31.72	30.31	0.95	noncompetitive
PMo_2	16.92	17.10	16.80	0.98	noncompetitive
PMo_3	18.27	19.20	18.90	0.98	noncompetitive
DPV	25.18	9.13	21.22	2.30	mixed inhibition
DMo_1	16.90	6.00	21.50	3.58	mixed inhibition
DMo_2	17.94	7.50	24.50	3.27	mixed inhibition
free polymer	- -	- -	- -	- -	- - - -

[a] Note: The ALP-catalyzed rates of hydrolysis of *p*-NPP at pH 10.0 were determined at 30 °C by measuring A_{405} in a reaction mixture containing ALP (3.3 μg/mL), *p*-NPP (2 mM) in incubation buffer (25 mM glycine + 2 mM $MgCl_2$, pH 10.0) in the presence of stated concentrations of the inhibitors. The V_{max} and K_m in the absence of inhibitor were found to be 7.9 μM/min and 2.85 mM, respectively. For polymeric compounds concentrations are on the basis of peroxometal loading.

the polymeric ligands, without peroxometal loading and the amino acid coligands viz. glycine and asparagine, upon ALP activity is practically negligible under the assay conditions used and H_2O_2 as such had no observable effect.

An inhibitor species can interact with an enzyme in various ways, and enzyme kinetics investigation is a major tool in enabling us to distinguish between the inhibition mechanisms of enzyme-catalyzed reactions. We determined kinetic parameters K_m and V_{max} in the absence as well as in the presence of peroxo metal compounds using Lineweaver−Burk double-reciprocal plots. Presented in Table 6 are the kinetic data for inhibition of ALP-catalyzed hydrolysis of *p*-NPP by the macrocomplexes as well as free **DPV** and mononuclear **DMo_1** and **DMo_2**. Kinetic measurements at several different substrate concentrations in the presence of each of the inhibitors yielded straight lines with a point of intersection in the second quadrant. Lineweaver−Burk plots obtained for compounds **PV_3**, **PMo_2**, **DPV**, and **DMo_1** are presented in Figure 9. With an increase in concentration of each of the polymeric inhibitor complexes, a decrease in velocity V_{max} was noted whereas K_m remained constant. In contrast, when **DPV** or any of the free pMo complexes was used as an inhibitor, it was found that with increasing inhibitor concentration V_{max} decreased whereas the K_m value increased (Figure 9). It has thus been established that the polymeric compounds are classical noncompetitive inhibitors of ALP. On the other hand, monomeric diperoxometallates **DPV**, **DMo_1**, and **DMo_2** served as a mixed type of inhibitor of the enzyme combining competitive and noncompetitive modes of inhibition.

The affinity of the enzyme for the inhibitor can be measured by inhibitor constants. The inhibitor constant K_i for the competitive part of inhibition was determined from the secondary plot of the slope of the primary plot ($1/V$ versus $1/[S]$) against the inhibitor concentration with the intercept on the inhibitor axis being $-K_i$ (Figure 9). The value of K_{ii}, inhibitor constant for noncompetitive inhibition, was obtained from a linear secondary plot of $1/V_{max}$ against the inhibitor concentration of each inhibitor, the

dx.doi.org/10.1021/ic200368g |*Inorg. Chem.* 2011, 50, 8046–8062

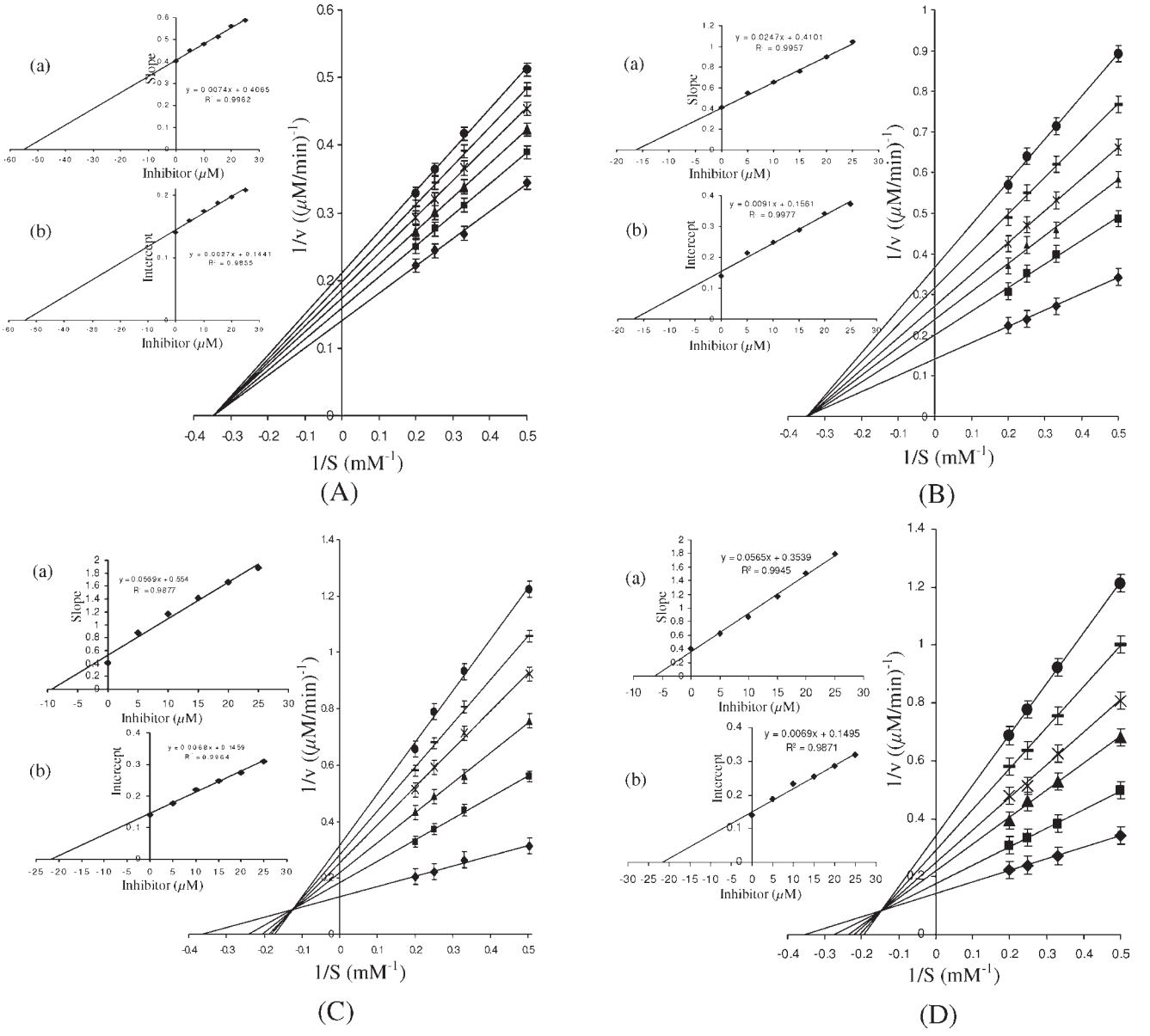

Figure 9. Lineweaver−Burk plots for inhibition of ALP activity in the absence and presence of (A) $\mathbf{PV_3}$, (B) $\mathbf{PMo_2}$, (C) **DPV**, and (D) $\mathbf{DMo_1}$. (Inset) Secondary plot of initial kinetic data of the Lineweaver plot. The reaction mixture contained glycine buffer (25 mM glycine + 2 mM $MgCl_2$, pH 10.0) and *p*-NPP (2−5 mM). The reaction was started by adding ALP (3.3 μg/mL) to the reaction solution which was preincubated for 5 min, and the rate of hydrolysis in the presence of (♦) 0, (■) 5, (▲) 10, (×) 15, (—) 20, and (●) 25 μM inhibitors was obtained. The values are expressed as means ± SE from three separate experiments. (Inset) (a) Slopes were plotted against inhibitor concentrations, and K_i values were obtained from the *x* intercepts of these replots. (b) Vertical intercepts were plotted against inhibitor concentration, and K_{ii} values were obtained from the *x* intercepts of these replots. For polymeric compounds concentrations are on the basis of peroxometal loading.

intercept on the inhibitor axis being equivalent to $-K_{ii}$ (Figure 9). The values of K_i and K_{ii} are presented in Table 6. For each of the macromolecular complexes the value of K_i was found to be equal to K_{ii}, which is typical of a noncompetitive inhibitor. For free diperoxovanadate as well as pMo complexes, $K_{ii} > K_i$, as is the case with a mixed type of inhibitor with a major mode of inhibition being of the competitive type.

Data obtained from similar experiments conducted with vanadate or molybdate showed these species to be competitive inhibitors of ALP, in agreement with previous reports.[1b,d,13a] The K_i values determined for vanadate and molybdate were 15 μM and 1.25 mM, respectively. It is apparent that vanadate is nearly 100 times stronger as an inhibitor of ALP compared to molybdate. A similar trend is observed on comparing inhibitor efficiencies of aqueous pV and pMo species. It is therefore intriguing to note that the affinity of the enzyme for the intact peroxomolybdenum compounds tested, irrespective of being neat or polymer bound, is almost double in magnitude in comparison to the peroxovanadate tested. These findings clearly demonstrate that there is a marked influence of the coligand environment on the inhibitory potency of the intact metal complexes as well as on the mode of their inhibition of the enzyme, although the effect of the individual ligand on the ALP activity is practically negligible under the assay conditions used.

dx.doi.org/10.1021/ic200368g |*Inorg. Chem.* 2011, 50, 8046–8062

It is particularly notable that the IC_{50} value of the peroxo metal species anchored PMA is nearly one-half of that of the corresponding poly(sodium acrylate)-anchored compounds in spite of these polymers having similar carboxylate functional groups as ligand sites. Pertinent here is to mention that the two compounds $\mathbf{PV_1}$ and $\mathbf{PV_2}$ earlier showed remarkable differences in their oxidant activity in oxidative bromination as well as their antibacterial properties.[16] Such variations in their tested chemical and biochemical properties may be ascribed to the difference in mode of coordination of the metal peroxo groups to the two polymers. In $\mathbf{PV_2}$ and $\mathbf{PMo_2}$ the diperoxo moieties are bound to the PMA chain exclusively in a monomeric fashion, whereas in $\mathbf{PV_1}$ and $\mathbf{PMo_1}$ the peroxo metals occur as dinuclear tetraperoxo species through bridging carboxylate groups of the PA chain. Consequently, the ionic charge distribution and polarity of the two compounds varies, and these factors are likely to influence their availability near the enzyme active site and their ability to interact with the enzyme to different extents.

It is known that a competitive inhibitor typically has close structural similarities to the normal substrate for the enzyme. The competitive inhibition of ALP by oxyanions of V, Mo, and W has been attributed to formation of pentacoordinated or hexacoordinated structures of these species, which are often described as phosphate analogues.[13,50] It has been observed earlier that the inhibitor potency of vanadium complexes depends on several factors such as the oxidation state of the metal, coordination geometry, stability of the compounds under physiological conditions, and nature of the phosphoproteins.[1d,9] Information available from the limited reports on the ALP inhibitory activity of synthetic pV compounds shows that a majority of the compounds tested were competitive inhibitors of the enzyme although there are examples of diperoxovanadate compounds showing mixed inhibition of Green-crab ALP, with K_i and K_{ii} values in the millimolar range.[14] It is pertinent here to mention that our recent investigation on a series of pW[18c,d] and pV[18e,51] compounds with amino acids and di- and tripeptides as ancillary ligands revealed that such compounds exert a mixed type of inhibition on the activity of ALP.

In the present study, structural analogy with the transition state or phosphate mimicry are unlikely to be the factors responsible for the noncompetitive mode of ALP inhibition exhibited by the polymer-anchored metal complexes mainly because of their macromolecular nature. A noncompetitive inhibitor usually binds reversibly at a site other than the active site and causes a change in the overall three-dimensional shape of the enzyme that leads to a decrease in catalytic activity. Due to the complexity of the reaction and species involved we are constrained in drawing any conclusion regarding the exact mechanism of inhibition of ALP by the compounds tested. Nevertheless, considering the reports documenting the importance of redox properties of peroxovanadium compounds in inhibition of protein phosphatases[1] in conjunction with our findings on the oxidant activity of some of these compounds such as bromide[15b,c,16] and glutathione(GSH) oxidant,[18c−e] it is reasonable to expect that the redox interaction of the intact macrocomplexes with the enzyme should be one of the likely causes of the observed inhibitory effect of the compounds on the phosphoproteins. It may be recalled that peroxovanadate effectively inhibited the tyrosine phophatase by oxidizing the critical cysteine residue in the catalytic domain of the enzyme.[1b,2c] Correlation has also been reported to exist between the GSH oxidizing ability and insulin mimetic activity of peroxo compounds of tungsten and molybdenum.[6] It is plausible that both factors, i.e., transition state analogy as well as oxidant activity of the pV or pMo species, would contribute to the mixed type of inhibition, combining competitive and noncompetitive pathways, exhibited by the hexacoordinated neat **DPV** complex as well as the monomeric heteroligand pV and pMo compounds.

CONCLUSIONS

The present investigation has established that it is possible to gain access to water-soluble, stable, and structurally defined peroxo metal-containing macromolecules by anchoring the metal peroxo species to appropriate polymer matrices. Undoubtedly, the most notable finding of the present study is that the polymer-anchored and free monomeric peroxo compounds tested induce their inhibitory effects on ALP through distinctly different pathways. Each of the macromolecular compounds tested is a noncompetitive inhibitor of ALP, in contrast to the free peroxo metal compounds which exert a mixed type of inhibition on the enzyme function. Remarkable features of the compounds, likely to be of clinical importance, include their hydrolytic stability in a wide range of pH values including acidic pH and their relative resistance to degradation by catalase. There is a search for peroxide derivatives easily formed and stable to degradation that can substitute for H_2O_2 at far lower doses without causing cytotoxicity to the normal cells, a great advantage in therapeutic application. It is hoped that the information obtained from the present study will help in identifying the right macroligand environment for peroxo metal derivatives to carry forward for in vivo studies.

ASSOCIATED CONTENT

Supporting Information. FTIR spectra and TG-DTG thermogram. This material is available free of charge via the Internet at http://pubs.acs.org.

AUTHOR INFORMATION

Corresponding Author

*Phone: +91-3712-267007. Fax:+91-3712-267006. E-mail: nsi@tezu.ernet.in.

ACKNOWLEDGMENT

Financial support from the Department of Science and Technology, New Delhi, India, is gratefully acknowledged. We are grateful to Prof. R. C. Deka, Department of Chemical Sciences, Tezpur University, for theoretical investigation. We thank Prof. T. Ramasarma, INSA Hon. Scientist, Indian Institute of Science (IISc), Bangalore, for valuable discussion, and Dr. S. Raghothama, Principal Research Scientist, NMR Research Centre, IISc, Bangalore, for the ^{95}Mo NMR spectra.

REFERENCES

(1) (a) Fantus, I. G.; Kodata, S.; Deregon, G.; Foster, B.; Posner, B. I. *Biochemistry* **1989**, *28*, 8864–8871. (b) Crans, D. C.; Smee, J. J.; Gaidamauskas, E.; Yang, L. *Chem. Rev.* **2004**, *104*, 849−902 and references therein. (c) Kustin, K. In *Vanadium Compounds: Chemistry, Biochemistry, and Therapeutic Applications*; Tracey, A. S., Crans, D. C., Eds.; Oxford University Press: New York, 1998; pp 170−185. (d) Crans, D. C. In *Vanadium Compounds: Chemistry, Biochemistry, and Therapeutic Applications*; Tracey,

A. S., Crans, D. C., Eds.; Oxford University Press: New York, 1998; pp 82−103.

(2) (a) Thompson, H. J.; Chasteen, N. D.; Meeker, L. D. *Carcinogenesis* **1984**, *5*, 849–851. (b) Djordjevic, C.; Wampler, G. L. *J. Inorg. Biochem.* **1985**, *25*, 51–55. (c) Tracey, A. S.; Willsky, G. R.; Takeuchi, E. S. *Vanadium: Chemistry, Biochemistry, Pharmacology and Practical Application*; CRC Press and Taylor & Francis Group: Boca Raton, 2007. (d) Jelikić-Stankov, M.; Uskoković-Marković, S.; Holclajtner-Antunović, I.; Todorović, M.; Djurdjević, P. *J. Trace Elem. Med. Biol.* **2007**, *21*, 8–16. (e) Butenko, N.; Tomaz, A. I.; Nouri, O.; Escribano, E.; Moreno, V.; Gama, S.; Ribeiro, V.; Telo, J. P.; Costa Pessoa, J.; Cavaco, I. *J. Inorg. Biochem.* **2009**, *103*, 622–632. (f) Rehder, D. *Inorg. Chem. Commun.* **2003**, *6*, 604–617. (g) Thompson, K. H.; Orvig, C. *J. Chem. Soc., Dalton Trans.* **2000**, 2885–2892.

(3) (a) Heyliger, C. E.; Tahiliani, A. G.; McNeill, J. H. *Science* **1985**, *227*, 1474–1477. (b) Thompson, K. H.; McNeill, J. H.; Orvig, C. *Chem. Rev.* **1999**, *99*, 2561–2572. (c) Shechter, Y.; Goldwaser, I.; Mironchik, M.; Fridkin, M.; Gefel, D. *Coord. Chem. Rev.* **2003**, *237*, 3–11. (d) Posner, B. I.; Faure, R.; Burgess, J. W.; Bevan, A. P.; Lachance, D.; Zhang-Sun, G.; Fantus, I. G.; Ng, J. B.; Hall, D. A.; Lum, B. S.; Shaver, A. *J. Biol. Chem.* **1994**, *269*, 4596–4604. (e) Ramasarma, T. In *Vanadium Biochemistry*; Alves, M. A., Ed.; Research Signpost: India, 2007; pp 45−76. (f) Ramasarma, T. *Proc. Indian Natn. Acad. Sci.* **2003**, *B69*, 649–672. (g) Thompson, K. H.; Lichter, J.; LeBel, C.; Scaife, M. C.; McNeill, J. H.; Orvig, C. *J. Inorg. Biochem.* **2009**, *103*, 554–558. (h) Bortolini, O.; Conte, V. *J. Inorg. Biochem.* **2005**, *99*, 1549–1557. (i) Kanamori, K.; Nishida, K.; Miyata, N.; Okamoto, K.; Miyoshi, Y.; Tamura, A.; Sakurai, H. *J. Inorg. Biochem.* **2001**, *86*, 649–656. (j) Srivastava, A. K. *Mol. Cell. Biochem.* **2000**, *206*, 177–182. (k) Rumora, L.; Hadzija, M.; Maysinger, D.; Zanic-Grubisic, T. *Cell Biol. Toxicol.* **2004**, *20*, 293–301. (l) Capella, M. A. M.; Capella, L. S.; Valente, R. C.; Gefe, M.; Lopes, A. G. *Cell Biol. Toxicol.* **2007**, *23*, 413–420. (m) Islam, Md. N.; Kumbhar, A. A.; Kumbhar, A. S.; Zeller, M.; Butcher, R. J.; Dusane, M. B.; Joshi, B. N. *Inorg. Chem.* **2010**, *49*, 8237–8246.

(4) Giorgio, M.; Trinei, M.; Migliaccio, E.; Pelicci, P. G. *Nat. Rev. Mol. Cell Biol.* **2007**, *8*, 722–728.

(5) Haldar, A. K.; Banerjee, S.; Naskar, K.; Kalita, D.; Islam, N. S.; Roy, S. *Exp. Parasitol.* **2009**, *122*, 145–154.

(6) Li, J.; Elberg, G.; Gefel, D.; Shechter, Y. *Biochemistry* **1995**, *34*, 6218–6225.

(7) (a) Waern, J. B.; Harding, M. M. *J. Organomet. Chem.* **2004**, *689*, 4655–4668. (b) Feliciano, I.; Matta, J.; Melendez, E. *J. Biol. Inorg. Chem.* **2009**, *14*, 1109–1117. (c) Kopf-Maier, P.; Klapotke, T. *J. Cancer Res. Clin. Oncol.* **1992**, *118*, 216–221.

(8) (a) Conte, V.; Floris, B. *Dalton Trans.* **2011**, *40*, 1419–1436. (b) Waidmann, C. R.; DiPasquale, A. G.; Mayer, J. M. *Inorg. Chem.* **2010**, *49*, 2383–2391. (c) Gabriel, C.; Kaliva, M.; Venetis, J.; Baran, P.; Rodriguez-Escudero, I.; Voyiatzis, G.; Zervou, M.; Salifoglou, A. *Inorg. Chem.* **2009**, *48*, 476–487.

(9) Louie, A. Y.; Meade, T. J. *Chem. Rev.* **1999**, *99*, 2711–2734.

(10) (a) Whyte, M. P. *Endocr. Rev.* **1994**, *15*, 439–461. (b) Holtz, K. M.; Kantrowitz, E. R. *FEBS Lett.* **1999**, *462*, 7–11. (c) Fennley, H. N. *The Enzymes*, 3rd ed.; Bouer, P. D., Ed.; Academic Press: New York, 1971; Vol. 4, pp 417−447.

(11) (a) Epstein, E.; Kiechle, F. L.; Ariss, J. D.; Zak, B. *Clin. Lab. Med.* **1986**, *6*, 491–505. (b) Li, M.; Ding, W.; Baruah, B.; Crans, D. C.; Wang, R. *J. Inorg. Biochem.* **2008**, *102*, 1846–1853. (c) Beck, G. R.; Sullivan, E. C., Jr.; Moran, E.; Zerler, B. *J. Cell. Biochem.* **1998**, *68*, 269–280.

(12) Vovk, A. I.; Kalchenko, V. I.; Cherenok, S. A.; Kukhar, V. P.; Muzychka, O. V.; Lozynsky, M. O. *Org. Biomol. Chem.* **2004**, *2*, 3162–3166.

(13) (a) Stankiewicz, P. J.; Gresser, M. J. *Biochemistry* **1988**, *27*, 206–212. (b) Heo, Y. S.; Ryu, J. M.; Park, S. M.; Park, J. H.; Lee, H. C.; Hwang, K. Y.; Kim, J. *Exp. Mol. Med.* **2002**, *34*, 211–223.

(14) (a) Zhou, X. W.; Chen, Q. X.; Chen, Z.; He, Z. Q.; Zhou, H. M. *Biochemistry (Moscow)* **2000**, *65*, 1424–1428. (b) Zhou, X. W.; Zhuang, Z. L.; Chen, Q. X. *J. Protein Chem.* **1999**, *18*, 735–740.

(15) (a) Djordjevic, C.; Vuletic, N.; Renslo, M. L.; Puryear, B. C.; Alimard, R. *Mol. Cell. Biochem.* **1995**, *153*, 25–29. (b) Sarmah, S.; Kalita, D.; Hazarika, P.; Borah, R.; Islam, N. S. *Polyhedron* **2004**, *23*, 1097–1107. (c) Sarmah, S.; Hazarika, P.; Islam, N. S.; Rao, A. V. S.; Ramasarma, T. *Mol. Cell. Biochem.* **2002**, *236*, 95–105.

(16) Kalita, D.; Sarmah, S.; Das, S. P.; Baishya, D.; Patowary, A.; Baruah, S.; Islam, N. S. *React. Funct. Polym.* **2008**, *68*, 876–890.

(17) (a) Butler, A. *Coord. Chem. Rev.* **1999**, *187*, 17–35. (b) Clague, M. J.; Butler, A. *J. Am. Chem. Soc.* **1995**, *117*, 3475–3484. (c) Colpas, G. J.; Hamstra, B. J.; Kampf, J. W.; Pecoraro, V. L. *J. Am. Chem. Soc.* **1996**, *118*, 3469–3478. (d) Conte, V.; Bortolini, O.; Carraro, M.; Moro, S. *J. Inorg. Biochem.* **2000**, *80*, 41–49. (e) Meister, G. E.; Butler, A. *Inorg. Chem.* **1994**, *33*, 3269–3275. (f) Butler, A.; Clague, M. J.; Meister, G. E. *Chem. Rev.* **1994**, *94*, 625–638.

(18) (a) Sarmah, S.; Hazarika, P.; Islam, N. S. *Polyhedron* **2002**, *21*, 389–394. (b) Hazarika, P.; Kalita, D.; Sarmah, S.; Borah, R.; Islam, N. S. *Polyhedron* **2006**, *25*, 3501–3508. (c) Hazarika, P.; Kalita, D.; Sarmah, S.; Islam, N. S. *Mol. Cell. Biochem.* **2006**, *284*, 39–47. (d) Hazarika, P.; Kalita, D.; Islam, N. S. *J. Enzym. Inhib. Med. Chem.* **2008**, *23*, 504–513. (e) Kalita, D.; Das, S. P.; Islam, N. S. *Biol. Trace Elem. Res.* **2009**, *128*, 200–219. (f) Hazarika, P.; Kalita, D.; Islam, N. S. *Inorg. Chem. Commun.* **2007**, *10*, 45–48.

(19) (a) Skorobogaty, A.; Smith, T. D. *Coord. Chem. Rev.* **1984**, *53*, 55–226. (b) Sherrington, D. C. *Pure Appl. Chem.* **1988**, *60*, 401–414. (c) Pomogalilo, A. D. *Catalysis by Polymer Immobilized Metal Complexes*; Gordon and Breach Scientific Publishers: Amsterdam, 1998. (d) Sherrington, D. C. *J. Polym. Sci. A: Polym. Chem.* **2001**, *39*, 2364–2377. (e) Choplin, A.; Quignard, F. *Coord .Chem. Rev.* **1998**, *180*, 1679–1702. (f) Sherrington, D. C. *Catal. Today* **2000**, *57*, 87–104. (g) McNamara, C. A.; Dixon, M. J.; Bradley, M. A. *Chem. Rev.* **2002**, *102*, 3275–3300. (h) Maurya, M. R.; Arya, A.; Kumar, A.; Kuznetsov, M. L.; Avecilla, F.; Pessoa, J. C. *Inorg. Chem.* **2010**, *49*, 6586–6600. (i) Chan, W. K. *Coord. Chem. Rev.* **2007**, *251*, 2104–2118. (j) Breslow, R.; Belvedere, S.; Gershell, L.; Leung, D. *Pure Appl. Chem.* **2000**, *72*, 333–342. (k) Schechter, B.; Arnon, R.; Wilchek, M. *React. Polym.* **1995**, *25*, 167–175.

(20) (a) Bergbreiter, D. E. *Chem. Rev.* **2002**, *102*, 3345–3384. (b) Dickerson, T. J.; Reed, N. N.; Janda, K. D. *Chem. Rev.* **2002**, *102*, 3325–3344.

(21) (a) Jagur-Grodzinski, J. *React. Funct. Polym.* **1999**, *39*, 99–138. (b) Avichezer, D.; Schechter, B.; Arnon, R. *React. Polym.* **1998**, *36*, 59–69. (c) Ohya, Y.; Masunaga, T.; Baba, T.; Ouchi, T. *J. Macromol. Sci. Pure Appl. Chem. A* **1996**, *33*, 1005–1016.

(22) (a) Nurkeeva, Z. S.; Khutoryanskiy, V. V.; Mun, G. A.; Sherbakova, M. V.; Ivaschenko, A. T.; Aitkhozhina, N. A. *Eur. J. Pharm. Biopharm.* **2004**, *57*, 245–249. (b) Fonseca, M. J.; Cabanes, A.; Alsina, M. A.; Reig, F. *Int. J. Pharm.* **1996**, *133*, 265–268. (c) Turos, E.; Shim, J. Y.; Wang, Y.; Greenhalgh, K.; Reddy, G. S. K.; Dickey, S.; Lim, D. V. *Bioorg. Med. Chem. Lett.* **2007**, *17*, 53–56.

(23) Garg, S.; Vermani, K.; Garg, A.; Anderson, R. A.; Rencher, W. B.; Zaneveld, L. J. D. *Pharm. Res.* **2005**, *22*, 584–595.

(24) Djordjevic, C.; Vuletic, N.; Jacobs, B. A.; Lee-Renslo, M.; Sinn, E. *Inorg. Chem.* **1997**, *36*, 1798–1805.

(25) Braun, D.; Cherdron, H.; Rehahn, M.; Ritter, H.; Voit, B. *Polymer Synthesis: Theory and Practice: Fundamentals, Methods, Experiments*, 4th ed.; Springer Berlin Heidelberg: New York, 2005; pp 176−177.

(26) Chaudhuri, M. K.; Ghosh, S. K.; Islam, N. S. *Inorg. Chem.* **1985**, *24*, 2706–2707.

(27) Bassett, J.; Denney, R. C.; Jeffery, G. H.; Mendham, J. *VOGEL's Textbook of Quantitative Inorganic Analysis including Elementary Instrumental Analysis*, 4th ed.; Longman Group Ltd.: London, 1978; pp 472−473.

(28) (a) Rivas, B. L.; Moreno-Villoslada, I. *J. Appl. Polym. Sci.* **1998**, *70*, 219–225. (b) Rivas, B. L.; Moreno-Villoslada, I. *J. Phys. Chem. B* **1998**, *102*, 6994–6999. (c) Rivas, B. L.; Moreno-Villoslada, I. *Chem. Lett.* **2000**, *29*, 166–167.

(29) (a) Dickman, M. H.; Pope, M. T. *Chem. Rev.* **1994**, *94*, 569–584. (b) Campbell, N. J.; Dengel, A. C.; Griffith, W. P. *Polyhedron* **1989**, *8*, 1379–1386. (c) Connor, J. A.; Ebsworth, E. A. V. *Adv. Inorg. Chem. Radiochem.* **1964**, *6*, 279–381.

(30) Lever, A. B. P.; Gray, H. B. *Acc. Chem. Res.* **1978**, *11*, 348–355.

(31) (a) Nakamoto, K. *Infrared and Raman Spectra of Inorganic and Co-ordination Compounds, Part B*, 5th ed.; Wiley and Sons: New York,

1997; p 60. (b) Deacon, G. B.; Phillips, R. J. *Coord. Chem. Rev.* **1980**, *33*, 227–250.
(32) (a) Djordjevic, C.; Lee, M.; Sinn, E. *Inorg. Chem.* **1989**, *28*, 719–723. (b) Schwendt, P.; Svancarek, P.; Kuchta, L.; Marek, J. *Polyhedron* **1998**, *17*, 2161–2166.
(33) (a) Li, H.; Tripp, C. P. *Langmuir* **2004**, *20*, 10526–10533. (b) Jones, F.; Farrow, J. B.; Van-Bronswijk, W. *Langmuir* **1998**, *14*, 6512–6517.
(34) (a) Feng, Y.; Schmidt, A.; Weiss, R. A. *Macromolecules* **1996**, *29*, 3909–3917. (b) Penland, R. B.; Mizushima, S.; Curran, C.; Quagliano, J. V. *J. Am. Chem. Soc.* **1957**, *79*, 1576–1578. (c) Bull, W. E.; Madan, S. K.; Willis, J. E. *Inorg. Chem.* **1963**, *2*, 303–306. (d) Murugan, R.; Mohan, S.; Bigotto, A. *J. Korean Phys. Soc.* **1998**, *31*, 505–512. (e) Silverstein, R. M.; Bassler, G. C.; Morrill, T. C. *Spectrometric identification of Organic Compounds*, 5th ed.; John Wiley and Sons: New York, 1991; p 122. (f) Silverstein, R. M.; Bassler, G. C.; Morrill, T. C. *Spectrometric identification of Organic Compounds*, 5th ed.; John Wiley and Sons: New York, 1991; p 129.
(35) (a) Rivas, B. L.; Seguel, G. V.; Geckeler, K. E. *J. Appl. Polym. Sci.* **2002**, *85*, 2546–2551. (b) Sun, Z. M.; Mao, J. G.; Sun, Y. Q.; Zeng, H. Y.; Clearfield, A. *Inorg. Chem.* **2004**, *43*, 336–341.
(36) Bayot, D.; Tinant, B.; Devillers, M. *Inorg. Chim. Acta* **2004**, *357*, 809–816.
(37) Van Dyke, J. D.; Kasperski, K. L. *J. Polym. Sci.: Polym. Chem.* **1993**, *31*, 1807–1823.
(38) (a) Grzywa, M.; Nitek, W.; Lasocha, W. *J. Mol. Struct.* **2008**, *888*, 318–326. (b) Djordjevic, C.; Lee-Renslo, M.; Sinn, E. *Inorg. Chim. Acta* **1995**, *233*, 97–102. (c) Kaliva, M.; Raptopoulou, C. P.; Terzis, A.; Salifoglou, A. *Inorg. Chem.* **2004**, *43*, 2895–2905. (d) Tsaramyrsi, M.; Kavousanaki, D.; Raptopoulou, C. P.; Terzis, A.; Salifoglou, A. *Inorg. Chim. Acta* **2001**, *320*, 47–59. (e) Campbell, N. J.; Dengel, A. C.; Edwards, C. J.; Griffith, W. P. *J. Chem. Soc., Dalton. Trans.* **1989**, 1203–1207. (f) Schwendt, P.; Tyrselova, J.; Pavelcik, F. *Inorg. Chem.* **1995**, *34*, 1964–1966. (g) Djordjevic, C.; Puryear, B. C.; Vuletic, N.; Abelt, C. J.; Sheffield, S. J. *Inorg. Chem.* **1988**, *27*, 2926–2932. (h) Stomberg, R.; Olson, S.; Svensson, I. B. *Acta Chem. Scand.* **1984**, *38A*, 653–656. (i) Justino, L. L. G.; Ramos, M. L.; Caldeira, M. M.; Gil, V. M. S. *Inorg. Chim. Acta* **2003**, *356*, 179–186. (j) Hou, S. Y.; Zho, Z. H.; Wan, H. L.; Ng, S. W. *Inorg. Chem. Commun.* **2003**, *6*, 1246–1248. (k) Schwendt, P.; Svancarek, P.; Kuchta, L.; Marek, J. *Polyhedron* **1998**, *17*, 2161–2166. (l) Ahmed, M.; Schwendt, P.; Marek, J.; Sivak, M. *Polyhedron* **2004**, *23*, 655–663. (m) Sarmah, S.; Islam, N. S. *J. Chem. Res. (S)* **2001**, 172–174.
(39) (a) Dengel, A. C.; Griffith, W. P.; Powell, R. D.; Skapski, A. C. *J. Chem. Soc., Dalton Trans.* **1987**, 991–995. (b) Jacobson, S. E.; Tang, R.; Mares, F. *Inorg. Chem.* **1978**, *17*, 3055–3063. (c) Pettersson, L.; Andersson, I.; Gorzsas, A. *Coord. Chem. Rev.* **2003**, *237*, 77–87. (d) Conte, V.; Furia, F. D.; Moro, S. *J. Mol. Catal.* **1994**, *94*, 323–333.
(40) (a) Bodor, A.; Banyai, I.; Toth, I. *Coord. Chem. Rev.* **2002**, *228*, 175–186. (b) Zhou, Z. H.; Deng, Y. F.; Cao, Z. X.; Zhang, R. H.; Chow, Y. L. *Inorg. Chem.* **2005**, *44*, 6912–6914. (c) Justino, L. L. G.; Ramos, M. L.; Caldeira, M. M.; Gil, V. M. S. *Inorg. Chim. Acta* **2000**, *311*, 119–125. (d) Matzapetakis, M.; Raptopoulou, C. P.; Terzis, A.; Lakatos, A.; Kiss, T.; Salifoglou, A. *Inorg. Chem.* **1999**, *38*, 618–619.
(41) Garces, F. O.; Sivadasan, K.; Somasundaran, P.; Turro, N. J. *Macromolecules* **1994**, *27*, 272–278.
(42) (a) Harrison, A. T.; Howarth, O. W. *J. Chem. Soc., Dalton Trans.* **1985**, 1173–1177. (b) Tracey, A. S.; Jaswal, J. S. *Inorg. Chem.* **1993**, *32*, 4235–4243. (c) Bortolini, O.; Carraro, M.; Conte, V.; Moro, S. *Eur. J. Inorg. Chem.* **1999**, 1489–1495. (d) Angus-Dunne, J. S.; Paul, P. C.; Tracey, A. S. *Can. J. Chem.* **1997**, *75*, 1002–1010. (e) Howarth, O. W.; Hunt, J. R. *J. Chem. Soc., Dalton Trans.* **1979**, 1388–1391. (f) Tracey, A. S.; Jaswal, J. S. *J. Am. Chem. Soc.* **1992**, *114*, 3835–3840.
(43) Nardello, V.; Marko, J.; Vermeersch, G.; Aubry, J. M. *Inorg. Chem.* **1995**, *34*, 4950–4957.
(44) Delly, B. *J. Chem. Phys.* **1990**, *92*, 508–514.
(45) Shisheva, A.; Ikonomov, O.; Shechter, Y. *Endocrinology* **1994**, *134*, 507–510.
(46) Goldstein, B. J.; Kalyankar, M.; Wu, X. *Diabetes* **2005**, *54*, 311–321.
(47) Rao, A. V. S.; Ravishankar, H. N.; Ramasarma, T. *Biochim. Biophys. Acta* **1998**, *1381*, 249–255.
(48) Ramasarma, T. *Ind. J. Clin. Biochem.* **1996**, *11*, 92–107.
(49) Ravishankar, H. N.; Rao, A. V. S.; Ramasarma, T. *Arch. Biochem. Biophys.* **1995**, *321*, 477–484.
(50) (a) Van-Etten, R. L.; Waymack, P. P.; Rehkop, D. M. *J. Am. Chem. Soc.* **1974**, *96*, 6782–6785. (b) Soman, G.; Chang, Y. C.; Graves, D. J. *Biochemistry* **1983**, *22*, 4994–5000.
(51) Hazarika, P.; Sarmah, S.; Kalita, D.; Islam, N. S. *Transition Met. Chem.* **2008**, *33*, 69–77.